Monolithic multigrid solvers for flow problems in porous media

Carmen Rodrigo (carmenr@unizar.es)

IUMA, Department of Applied Mathematics, University of Zaragoza

Departamento de Matemática Aplicada
Universidad Zaragoza

Instituto Universitario de Investigación de Matemáticas y Aplicaciones
Universidad Zaragoza

2021 CRM SUMMER SCHOOL

Solving large systems efficiently in multiphysics numerical simulations

May 31-June 10, 2021

Outline

MONOLITHIC MULTIGRID SOLVERS

- Flow problems in deformable porous media
- Coupled flow and porous media problems (Stokes-Darcy and Stokes-Biot)
- Flow problems in fractured porous media

Poroelasticity problem. Introduction

- A deformable porous material consists of an elastic matrix containing interconnected fluid-saturated pores.
- In physical terms, when a porous material is subjected to stress, the resulting matrix deformation leads to volumetric changes in the pores.
- Since the pores are fluid-filled, the presence of the fluid results in the flow of the pore fluid between regions of higher and lower pore pressure.
- The theory of poro-elasticity addresses the time dependent coupling between the deformation of a porous material and the fluid flow inside it.

Poroelasticity problem. Subsidence

SUBSIDENCE from groundwater pumping in San Joaquin Valley (California)

Courtesy of California Department of Water Resources

Poroelasticity problem. Subsidence

SUBSIDENCE from groundwater pumping in San Joaquin Valley (California)

Courtesy of California Department of Water Resources

Poroelasticity problem. Subsidence

SUBSIDENCE from groundwater pumping in San Joaquin Valley (California)

Courtesy of California Department of Water Resources

Poroelasticity problem

QUASI-STATIC BIOT'S MODEL:

Equilibrium equation: $\operatorname{div} \boldsymbol{\sigma}' - \alpha \nabla p = \rho \mathbf{g}, \quad \text{in } \Omega,$

(or equivalently $\operatorname{div} \boldsymbol{\sigma} = \rho \mathbf{g},\ \boldsymbol{\sigma} = \boldsymbol{\sigma}' - \alpha \mathbf{I} p$)

Generalized form of Hooke's law: $\boldsymbol{\sigma}' = \lambda \operatorname{tr}(\boldsymbol{\epsilon}) \mathbf{I} + 2\mu \boldsymbol{\epsilon}, \quad \text{in } \Omega,$

Compatibility equation: $\boldsymbol{\epsilon}(\mathbf{u}) = \frac{1}{2}(\nabla \mathbf{u} + \nabla \mathbf{u}^t), \quad \text{in } \Omega.$

Darcy's law: $$\mathbf{w} = -\frac{1}{\mu_f} K (\nabla p - \rho_f \mathbf{g}), \quad \text{in } \Omega,$$

Continuity equation: $$\frac{\partial}{\partial t}\left(\frac{1}{M} p + \alpha \nabla \cdot \mathbf{u}\right) + \nabla \cdot \mathbf{w} = f, \quad \text{in } \Omega.$$

- λ and μ: Lamé coefficients
- α: Biot-Willis constant and M: Biot's modulus
- K: Permeability of the porous medium and ρ: density of the solid
- μ_f: viscosity of the fluid and ρ_f: density of the fluid
- $\mathbf{u}$: displacement vector and p: pore pressure
- $\boldsymbol{\sigma}'$ and $\boldsymbol{\epsilon}$: effective stress and strain tensors
- $\mathbf{w}$: velocity of the fluid relative to the soil
- f: a forced fluid extraction or injection process and $\mathbf{g}$: gravity vector

Poroelasticity problem

Two-field (displacement-pressure) formulation

$$
\begin{aligned}
&-\nabla(\lambda+\mu)\nabla\cdot\mathbf{u} - \nabla\cdot\mu\nabla\mathbf{u} + \alpha\,\nabla\,p = \rho\mathbf{g},\\
&\frac{1}{M}\frac{\partial p}{\partial t} + \alpha\frac{\partial}{\partial t}(\nabla\cdot\mathbf{u}) - \nabla\cdot\left(\frac{1}{\mu_f}K(\nabla p - \rho_f\mathbf{g})\right) = f.
\end{aligned}
$$

Three-field (fluid velocity) formulation

$$
\begin{aligned}
&-\nabla(\lambda+\mu)\nabla\cdot\mathbf{u} - \nabla\cdot\mu\nabla\mathbf{u} + \alpha\,\nabla\,p = \rho\mathbf{g},\\
&K^{-1}\mu_f\mathbf{w} + \nabla p = \rho_f\mathbf{g},\\
&\frac{1}{M}\frac{\partial p}{\partial t} + \alpha\frac{\partial}{\partial t}(\nabla\cdot\mathbf{u}) + \nabla\cdot\mathbf{w} = f.
\end{aligned}
$$

Poroelasticity problem - Many Applications!

Reservoir Engineering

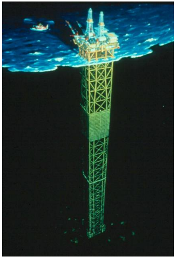

Bioengineering

Earthquake Engineering

Carbon Dioxide Storage

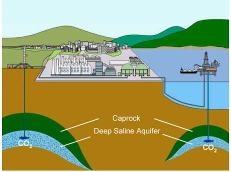

Hydraulic Fracturing

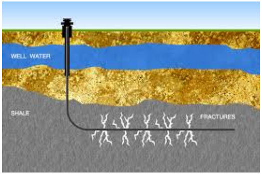

Animal Cells

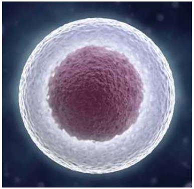

Poroelasticity problem - Many Applications!

Reservoir Engineering

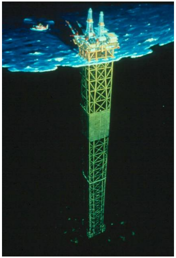

Bioengineering

Earthquake Engineering

Large variation of model parameters in many practical problems !!

Carbon Dioxide Storage

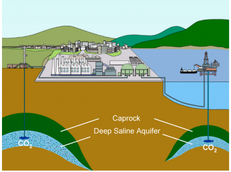

Hydraulic Fracturing

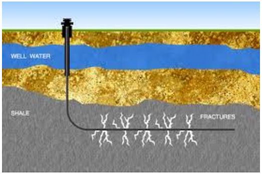

Animal Cells

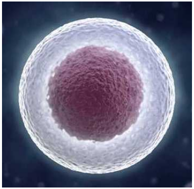

Poroelasticity problem. Discretization schemes

- Finite Difference schemes

  - F.J. Gaspar, F.J. Lisbona, P.N. Vabishchevich, A Finite Difference Analysis of Biot's Consolidation Model. Applied Numerical Mathematics, 44 (2003) 487-506.

  - F.J. Gaspar, F.J. Lisbona, P.N. Vabischevich, Staggered grid discretizations for the quasi-static Biot's consolidation problem, Applied Numerical Mathematics 56 (2006) pp. 888-898.

- Finite Volume methods

  - R.E. Ewing, O.P. Iliev, R.D. Lazarov, and A. Naumovich, On convergence of certain finite volume difference discretizations for 1-D poroelasticity interface problems, Numerical Methods for Partial Differential Equations 23 (3) (2007), 652-671.

  - J. M. Nordbotten, Stable cell-centered finite volume discretization for Biot equations, SIAM Journal on Numerical Analysis 54 (2) (2016) 942-968.

- Finite Element discretizations

  - M.A. Murad, V. Thomée, A.F.D. Loula, Asymptotic behavior of semidiscrete finite-element approximations of Biot's consolidation problem, SIAM J. Numer. Anal. 33 (1996) 1065-1083.

  - G. Aguilar, F. Gaspar, F. Lisbona, C. Rodrigo, Numerical stabilization of Biot's consolidation model by a perturbation on the flow equation, Internat. J. Numer. Methods Engrg. 75 (2008) 1282-1300.

  - C. Rodrigo, F.J. Gaspar, X. Hu, L.T. Zikatanov, Stability and monotonicity for some discretizations of the Biot's consolidation model, Computer Methods in Applied Mechanics

Poroelasticity problem. Robust discretization schemes

Search for parameter-robust stable discretizations

- J.J. Lee, Robust error analysis of coupled mixed methods for Biot's consolidation model, Journal of Scientific Computing 69 (2016) 610-632.
- J.J. Lee, K.-A. Mardal, and R. Winther. Parameter-robust discretization and preconditioning of Biot's consolidation model. SIAM Journal on Scientific Computing, 39 (2017) A1-A24.
- J. Adler, F.j. Gaspar, X. Hu, C. Rodrigo, L.T. Zikatanov, Robust Block Preconditioners for Biot's Model, Domain Decomposition Methods in Science and Engineering XXIV in Lecture Notes in Computational Science and Engineering, Vol. 125, Bjostad, P.E., Brenner, S.C., Halpern, L., Kim, H.H., Kornhuber, R., Rahman, T., Widlund, O.B. (Eds.), 2018.
- Q. Hong, J. Kraus, Parameter-robust stability of classical three-field formulation of Biot's consolidation model, ETNA, 48 (2018) 202-226.

Standard discretizations in space give nonphysical oscillations in the solution of the pressure.

Terzaghi's problem

$$-\frac{\partial}{\partial x}\left((\lambda+2\mu)\frac{\partial u}{\partial x}\right)+\frac{\partial p}{\partial x}=0, \quad x\in(0,1),$$

$$\frac{\partial}{\partial t}\left(\frac{\partial u}{\partial x}\right)-\frac{\partial}{\partial x}\left(\frac{\kappa}{\eta}\frac{\partial p}{\partial x}\right)=0.$$

$$(\lambda+2\mu)\frac{\partial u}{\partial x}=-1, \quad p=0, \qquad x=0,$$

$$u=0, \quad \frac{\partial p}{\partial x}=0, \qquad x=1,$$

$$\frac{\partial u}{\partial x}=0, \quad x\in(0,1), \quad t=0.$$

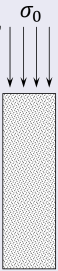

P1-P1 + Implicit Euler

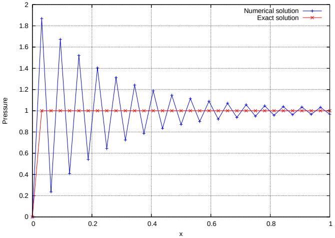

Poroelasticity problem. Numerical difficulties

Standard discretizations in space give nonphysical oscillations in the solution of the pressure.

Terzaghi's problem

$$-\frac{\partial}{\partial x}\left((\lambda+2\mu)\frac{\partial u}{\partial x}\right)+\frac{\partial p}{\partial x}=0,\quad x\in(0,1),$$

$$\frac{\partial}{\partial t}\left(\frac{\partial u}{\partial x}\right)-\frac{\partial}{\partial x}\left(\frac{\kappa}{\eta}\frac{\partial p}{\partial x}\right)=0.$$

$$(\lambda+2\mu)\frac{\partial u}{\partial x}=-1,\quad p=0,\qquad x=0,$$

$$u=0,\quad \frac{\partial p}{\partial x}=0,\qquad x=1,$$

$$\frac{\partial u}{\partial x}=0,\quad x\in(0,1),\quad t=0.$$

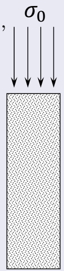

P1-P1 + Implicit Euler

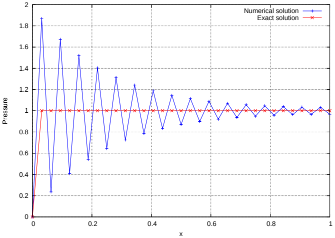

MINI + Implicit Euler

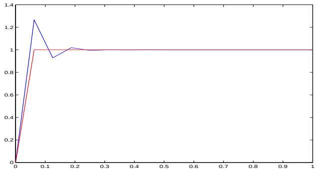

Poroelasticity problem. Numerical difficulties

LAYERED POROUS MEDIUM WITH VARIABLE PERMEABILITY

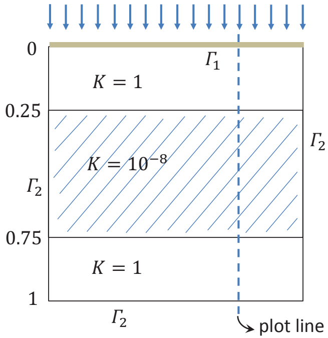

$$p = 0, \qquad \boldsymbol{\sigma} \cdot \mathbf{n} = \mathbf{g}, \text{ with } \mathbf{g} = (0, -1)^t, \text{ on } \Gamma_1$$
$$\nabla p \cdot \mathbf{n} = 0, \qquad \mathbf{u} = \mathbf{0}, \text{ on } \Gamma_2$$

P1–P1

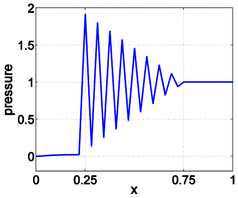

P1–P1 + stab

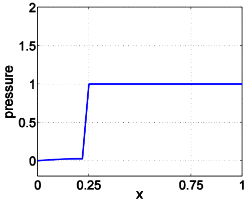

Poroelasticity problem. Numerical difficulties (FEM)

Table from *"On the causes of pressure oscillations in low-permeable and low-compressible porous media"* by J. Haga, H. Osnes and H. Langtangen.

$\mathbf{u}$	p_s	$\mathbf{w}$	p	Test 1	Test 2	Test 3
P_1	–	–	P_1	Fail	Fail	Fail
P_2	–	–	P_2	Fail	Fail	Fail
P_1^+	–	–	P_1	OK*	OK*	OK*
P_2	–	–	P_1	OK*	OK*	OK*
P_2	–	RT_1	P_0	OK	OK	OK
P_2	–	P_2	P_1	OK*	OK*	OK*
P_2^+	–	P_2^+	P_{-1}	OK	OK	OK
P_1^+	P_1	–	P_1	OK*	OK*	OK
P_1^+	P_1	RT_1	P_0	Fail	Fail	Fail
P_2^+	P_{-1}	RT_1	P_0	OK	OK	OK
P_2	P_0	RT_1	P_0	OK	OK	OK
P_2^+	P_{-1}	P_2^+	P_{-1}	OK	OK	OK

DESIRABLE PROPERTIES

- Free of non-physical oscillations (MONOTONICITY?)
- Uniform stability with respect to the discretization and physical parameters

Discretizations. FEM for the two-field formulation

FEM for the two-field formulation

We consider the discretization of poroelasticity problem given by operators of the form $\mathcal{A}_C = \begin{pmatrix} A & B' \\ B & -C \end{pmatrix}$, where C is bounded, selfadjoint and positive definite.

$\mathcal{A}_C$ is an isomorphism $\Leftrightarrow$ For any $q \in \mathcal{Q}_h^{k'}$, $\sup\limits_{v \in \mathcal{U}_h^k} \dfrac{\langle B\, v, q \rangle}{\| v \|_A} \geq \gamma_B \| q \| - \| q \|_C$

If inf-sup condition for B is satisfied with $C = 0$,
then it is also satisfied with $C > 0$

Stable finite element pair for Stokes is also stable for poroelasticity

C. Rodrigo, F.J. Gaspar, X. Hu, L.T. Zikatanov, Stability and monotonicity for some discretizations of the Biot's consolidation model, Computer methods in applied mechanics and engineering, 2016

- P1-P1 + Stabilization
- MINI element + Stabilization

DESIRABLE PROPERTIES

- Robust convergence with respect to the discretization and physical parameters.
- Efficient.

DESIRABLE PROPERTIES

- Robust convergence with respect to the discretization and physical parameters.
- Efficient.

Mainly two approaches:

- Iterative coupling methods: solve sequentially the equations for fluid flow and geomechanics until a converged solution is achieved.
  - Flexibility: two different codes for fluid flow and geomechanics can be linked for solving the poroelastic problems.
  - Most frequently used: fixed-stress split method.

    J. Kim, H.A. Tchelepi, R. Juanes, Stability, Accuracy, and Efficiency of Sequential Methods for Coupled Flow and Geomechanics. Society of Petroleum Engineers (2011)

    A. Mikelic, M.F. Wheeler, Convergence of iterative coupling for coupled flow and geomechanics, Comput. Geosci. (2013)

    J. Both, M. Borregales, J.M. Nordbotten, K. Kumar, F. Radu, Robust fixed stress splitting for Biot's equations in heterogeneous media, Applied Mathematics Letters. (2017)
- Monolithic or fully coupled methods: the linear system is solved simultaneously for all the unknowns.

MONOLITHIC APPROACHES

- Preconditioners for Krylov subspace methods
  - L. Bergamaschi, M. Ferronato, G. Gambolati, Novel preconditioners for the iterative solution to FE-discretized coupled consolidation equations, Comput. Methods Appl. Mech. Engrg. 196 (25) (2007) 2647-2656.
  - M. Ferronato, L. Bergamaschi, G. Gambolati, Performance and robustness of block constraint preconditioners in finite element coupled consolidation problems, Internat. J. Numer. Methods Engrg. 81 (2010) 381-402.
  - N. Castelleto, J.A. White, H.A. Tchelepi, Accuracy and convergence properties of the fixed-stress iterative solution of two-way coupled poromechanics, Int. J. Numer. Anal. Methods Geomech. 39 (2015) 1593-1618.
  - J.J. Lee, K.-A. Mardal, and R. Winther, Parameter-robust discretization and preconditioning of Biot's consolidation model. SIAM Journal on Scientific Computing, 39 (2017) A1-A24.
  - J.H. Adler, F.J. Gaspar, X. Hu, P. Ohm, C. Rodrigo, and L.T. Zikatanov, Robust preconditioners for a new stabilized discretization of the poroelastic equations, SIAM Journal on Scientific Computing, 42 (3) (2020) B761-B791.
  - M. Ferronato, A. Franceschini, C. Janna, N. Castelletto, and H. A. Tchelepi, A general preconditioning framework for coupled multiphysicsproblems with application to contact-and poro-mechanics, Journal of Computational Physics 398 (2019), 108887.
- Monolithic multigrid methods (design of the smoother)

  ➡ In this talk

Monolithic Multigrid

- Convergence factor independent of the discretization parameter.
- Computational cost $\mathcal{O}(n)$.
- For dealing with complex domains:

SEMI-STRUCTURED GRIDS + GEOMETRIC MG

Hierarchy of grids:

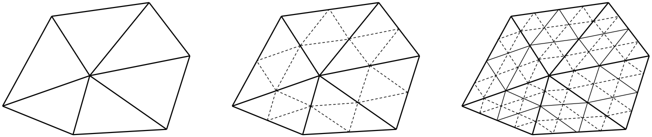

- Unstructured initial grid: Adequately represent the domain geometry.
- Structured patches: Efficient implementation of geometric multigrid based on stencil-based operations. Free-matrix code.

B. Bergen, T. Gradl, F. Hülsemann, U. Rüde. A massively parallel multigrid method for finite elements. Comput. Sci. Eng., 2006.

C. Rodrigo, Geometric Multigrid Methods on Semi-Structured Triangular Grids, PhD thesis, University of Zaragoza, 2010

Local Fourier Analysis (LFA)

LOCAL FOURIER ANALYSIS

Main quantitative analysis for multigrid methods
To estimate the spectral radius of the k–grid operator which are quantitative measures for the error reduction.

- Based on the Fourier transform theory.
- Very powerful tool for the design of new efficient multigrid methods.
- Classically, LFA provides exact convergence rates of GMG on rectangular domains with periodic boundary conditions.
- Recently, it has been proved that LFA yields the exact convergence factors for a wider class of problems.

  C. Rodrigo, F.J. Gaspar, L.T. Zikatanov, On the validity of the Local Fourier Analysis, J. Comp. Math., 37 (2019), pp. 340-348.

Monolithic Multigrid for saddle point problems

COUPLED OR VANKA SMOOTHERS: Decomposing the mesh into small subdomains and simultaneously solve all the equations in each block

F.J.. Gaspar, F.J. Lisbona, C.W. Oosterlee, A stabilized difference scheme for deformable porous media and its numerical resolution by multigrid methods, Computing and Visualization in Science, 2008

C. Rodrigo, Geometric Multigrid Methods on Semi-Structured Triangular Grids, PhD Thesis, University of Zaragoza, 2010

DECOUPLED SMOOTHERS:

- Distributive: Transform the discrete system, smooth such system equation-wise, perform a back-transformation to the original unknowns

  R. Wienands, F.J. Gaspar, F.J. Lisbona, C.W. Oosterlee, An efficient multigrid solver based on distributive smoothing for poroelasticity equations, Computing, 2004

- Uzawa: Standard smoothing process for the displacements and updating of pressure by a Richardson iteration with an appropriate parameter ω

  F.J. Gaspar, Y. Notay, C.W. Oosterlee, C. Rodrigo, A simple and efficient segregated smoother for the discrete Stokes equations. SIAM Journal on Scientific Computing, 2014

  P. Luo, C. Rodrigo, F.J. Gaspar, C.W. Oosterlee, On an Uzawa smoother in multigrid for poroelasticity equations, Numerical Linear Algebra with Applications, 2017

- Fixed-stress split smoother: Based on the iterative coupling fixed-stress split method.

  F.J. Gaspar, C. Rodrigo, On the fixed-stress split scheme as smoother in multigrid methods for coupling flow and geomechanics, Computer Methods in Applied Mechanics and Engineering, 2017

The fixed-stress split method

The fixed-stress split method is an iterative method where the flow problem is solved first supposing a constant volumetric mean total stress, $\sigma_v = tr(\sigma)/3$. By using $\sigma_v = K_b \nabla \cdot \mathbf{u} - \alpha p$, where $K_b = \lambda + 2\mu/d$ is the drained bulk modulus, we write the flow equation

$$\frac{1}{M}\frac{\partial p}{\partial t} + \alpha \frac{\partial}{\partial t}(\nabla \cdot \mathbf{u}) - \nabla \cdot \left(\frac{1}{\mu_f} \boldsymbol{K} \left(\nabla p - \rho_f \boldsymbol{g} \right) \right) = f.$$

in terms of the volumetric mean total stress instead of the volumetric strain,

$$\left(\frac{1}{M} + \frac{\alpha^2}{K_b} \right) \frac{\partial p}{\partial t} + \frac{\alpha}{K_b} \frac{\partial \sigma_v}{\partial t} - \nabla \cdot \left(\frac{1}{\mu_f} \boldsymbol{K} \left(\nabla p - \rho_f \boldsymbol{g} \right) \right) = f.$$

The fixed-stress split scheme is based on solving the flow equation considering known the volumetric mean total stress. In the discrete case, this is equivalent to an iterative method based on the splitting of matrix $\mathcal{A}$ as

$$\begin{bmatrix} A & B^T \\ B & -C \end{bmatrix} = \begin{bmatrix} A & B^T \\ 0 & -C + \frac{\alpha^2}{K_b} M_p \end{bmatrix} - \begin{bmatrix} 0 & 0 \\ -B & \frac{\alpha^2}{K_b} M_p \end{bmatrix},$$

where M_p is the mass matrix.

Fixed-stress split smoother

Decoupled smoother in a multigrid framework combining the advantages of being a fully-coupled method and the decoupling the flow and the mechanic part in the smoothing procedure.

Consider the splitting $\mathcal{A} = \mathcal{M}_A - \mathcal{N}_A = \begin{bmatrix} A & B^T \\ 0 & -C + LM_p \end{bmatrix} - \begin{bmatrix} 0 & 0 \\ -B & LM_p \end{bmatrix}$

Iterative method based on the splitting reads:

$$\begin{bmatrix} u_{k+1} \\ p_{k+1} \end{bmatrix} = \begin{bmatrix} u_k \\ p_k \end{bmatrix} + \mathcal{M}_A^{-1} \left(\begin{bmatrix} g \\ f \end{bmatrix} - \mathcal{A} \begin{bmatrix} u_k \\ p_k \end{bmatrix} \right)$$

Relaxation procedure:

$$\widetilde{\mathcal{M}_A} = \begin{bmatrix} M_A & B^T \\ 0 & M_S \end{bmatrix}$$

where

- M_A and M_S are suitable smoothers for operators A and $S = -C + LM_p$

$$\begin{cases} p_{k+1} = p_k + M_S^{-1} \left(g - Bu_k + Cp_k \right) \\ u_{k+1} = u_k + M_A^{-1} \left(f - Au_k - B^T p_{k+1} \right) \end{cases}$$

Fixed-stress split smoother

$$\widetilde{\mathcal{M}}_{A,T1} = \begin{bmatrix} M_A & B^T \\ 0 & M_S \end{bmatrix}, \quad \begin{cases} M_A = (D_A + L_A) D_A^{-1} (D_A + U_A), \\ M_S = (D_R + L_R) D_R^{-1} (D_R + U_R), R = -C + LM_p \end{cases}$$

Fixed-stress split smoother

$$\widetilde{\mathcal{M}}_{A,T1} = \begin{bmatrix} M_A & B^T \\ 0 & M_S \end{bmatrix}, \quad \begin{cases} M_A = (D_A + L_A) D_A^{-1} (D_A + U_A), \\ M_S = (D_R + L_R) D_R^{-1} (D_R + U_R), R = -C + L M_p \end{cases}$$

$$\widetilde{\mathcal{M}}_{A,T2} = \begin{bmatrix} M_A & B^T \\ 0 & M_S \end{bmatrix}, \quad \begin{cases} M_{A,1} = (D_A + L_A) D_A^{-1} (D_A + U_A), \\ M_A = M_{A,1} (2 M_{A,1} - A)^{-1} M_{A,1}, \\ M_S = (D_R + L_R) D_R^{-1} (D_R + U_R), R = -C + L M_p \end{cases}$$

Fixed-stress split smoother

$$\widetilde{\mathcal{M}}_{A,T1} = \left[\begin{array}{cc} M_A & B^T \\ 0 & M_S \end{array} \right], \quad \left\{ \begin{array}{l} M_A = (D_A + L_A) D_A^{-1} (D_A + U_A), \\ M_S = (D_R + L_R) D_R^{-1} (D_R + U_R), R = -C + L M_p \end{array} \right.$$

$$\widetilde{\mathcal{M}}_{A,T2} = \left[\begin{array}{cc} M_A & B^T \\ 0 & M_S \end{array} \right], \quad \left\{ \begin{array}{l} M_{A,1} = (D_A + L_A) D_A^{-1} (D_A + U_A), \\ M_A = M_{A,1} (2 M_{A,1} - A)^{-1} M_{A,1}, \\ M_S = (D_R + L_R) D_R^{-1} (D_R + U_R), R = -C + L M_p \end{array} \right.$$

$$\widetilde{\mathcal{M}}_{A,D2} = \left[\begin{array}{cc} M_A & 0 \\ 0 & M_S \end{array} \right], \quad \left\{ \begin{array}{l} M_{A,1} = (D_A + L_A) D_A^{-1} (D_A + U_A), \\ M_A = M_{A,1} (2 M_{A,1} - A)^{-1} M_{A,1}, \\ M_S = (D_R + L_R) D_R^{-1} (D_R + U_R), R = -C + L M_p \end{array} \right.$$

LFA results. Fixed-stress split smoother

Comparison between the two-grid analysis convergence factors predicted by LFA ρ and the experimentally computed asymptotic convergence factors ρ_h, for different numbers of smoothing steps, two different regular triangular grids (right and equilateral) and $K = 10^{-3}$

	ν	$\mathcal{M}_{A,T1}$	$\mathcal{M}_{A,T2}$	$\mathcal{M}_{A,D2}$
Right	1	0.45 (0.46)	0.28 (0.29)	0.28 (0.29)
	2	0.28 (0.29)	0.16 (0.17)	0.16 (0.16)
	3	0.20 (0.21)	0.12 (0.12)	0.12 (0.12)
	4	0.16 (0.17)	0.08 (0.09)	0.08 (0.09)
Equilateral	1	0.35 (0.35)	0.17 (0.17)	0.17 (0.17)
	2	0.13 (0.14)	0.05 (0.06)	0.05 (0.06)
	3	0.08 (0.08)	0.03 (0.04)	0.03 (0.04)
	4	0.05 (0.06)	0.02 (0.03)	0.02 (0.03)

LFA results. Fixed-stress split smoother

Two-grid analysis convergence factors predicted by LFA for different values of parameter K, by using different numbers of smoothing steps, and considering two different uniform triangular grids (right and equilateral)

		Right			Equilateral		
	$\nu \setminus K$	1	10^{-3}	10^{-6}	1	10^{-3}	10^{-6}
$\mathcal{M}_{A,T1}$	1	0.45	0.45	0.45	0.35	0.35	0.35
	2	0.28	0.28	0.28	0.13	0.13	0.13
	3	0.20	0.20	0.20	0.08	0.08	0.08
	4	0.16	0.16	0.16	0.05	0.05	0.05
$\mathcal{M}_{A,T2}$	1	0.28	0.28	0.28	0.17	0.17	0.17
	2	0.16	0.16	0.16	0.05	0.05	0.05
	3	0.12	0.12	0.12	0.03	0.03	0.03
	4	0.08	0.08	0.08	0.02	0.02	0.02
$\mathcal{M}_{A,D2}$	1	0.28	0.28	0.28	0.17	0.17	0.17
	2	0.16	0.16	0.16	0.05	0.05	0.05
	3	0.12	0.12	0.12	0.03	0.03	0.03
	4	0.08	0.08	0.08	0.02	0.02	0.02

Numerical experiment. Poroelastic footing problem

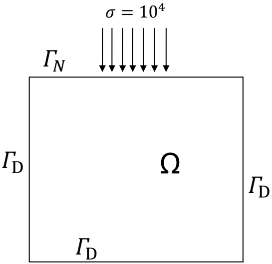

$$\begin{aligned}
\mathbf{u} = \mathbf{0}, &\quad \textit{on} \quad \Gamma_D \\
\sigma_{xy} = 0,\ \sigma_{yy} = -\sigma_0, &\quad \textit{on} \quad \Gamma_N \\
p = 0, &\quad \textit{on} \quad \Gamma_N \\
(\nabla p) \cdot \mathbf{n} = 0, &\quad \textit{on} \quad \Gamma_D
\end{aligned}$$

where

$$\sigma_0 = \begin{cases} \sigma = 10^4, & \text{on the ``central'' part of } \Gamma_N \\ 0, & \text{on the rest of } \Gamma_N \end{cases}$$

Numerical example. Poroelastic footing problem

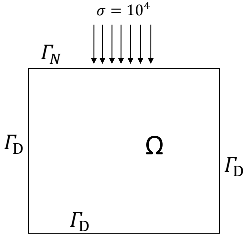

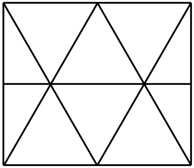

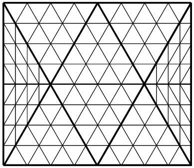

- Constant permeability

$\tau K/\mu_f$	6 levels	7 levels	8 levels	9 levels	10 levels
10^{-2}	11	11	11	11	11
10^{-4}	11	11	11	11	11
10^{-6}	11	11	11	11	11
10^{-8}	10	11	11	11	11
10^{-10}	12	11	10	10	11
10^{-12}	12	12	12	12	12

Numerical example. Poroelastic footing problem

- Two-layered porous medium

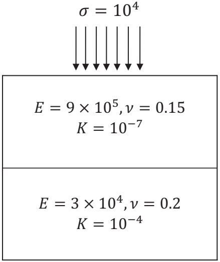

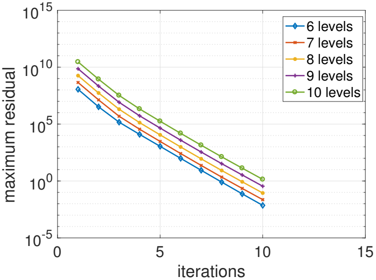

- Random heterogeneous materials (the permeability is modeled as a lognormal random field)

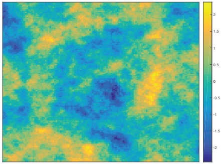

$\rho^{average} = 0.11$

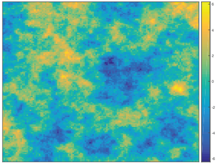

$\rho^{average} = 0.33$

Numerical experiment. Poroelasticity on a cylindrical shell

- POROELASTICITY ON A CYLINDRICAL SHELL

Poroelasticity equations

$$-\nabla(\lambda+\mu)\nabla\cdot\mathbf{u}-\nabla\cdot\mu\nabla\mathbf{u}+\nabla p=\rho\mathbf{g}$$

$$\frac{\partial}{\partial t}(\nabla\cdot\mathbf{u})-\nabla\cdot\left(\frac{K}{\mu_f}(\nabla p-\rho_f\mathbf{g})\right)=f(\mathbf{x},t)$$

Outer boundary:

$$\begin{aligned}\mathbf{u}&=0\\ \frac{K}{\mu_f}(\nabla p-\rho_f\mathbf{g})\cdot\mathbf{n}&=0\end{aligned}$$

Inner boundary:

$$\begin{aligned}\boldsymbol{\sigma}\cdot\mathbf{n}&=(\cos\theta,\sin\theta)\\ p&=1\end{aligned}$$

Geometry and boundary conditions:

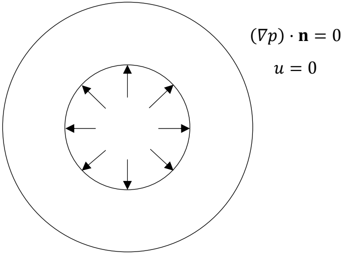

Material parameters:

Property	Value	Unit
Young's modulus	3×10^4	N/m^2
Poisson's ratio	0.2	-
Permeability: K	10^{-7}	m^2
Fluid viscosity: μ_f	10^{-3}	Pas
K/μ_f	10^{-4}	$m^2/$Pas

Numerical experiment. Poroelasticity on a cylindrical shell

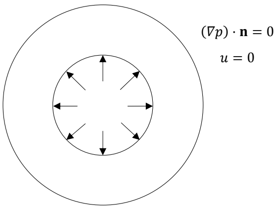

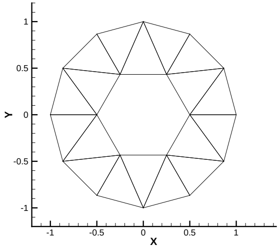

Coarsest triangulation

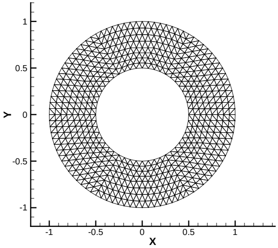

Grid after 4 ref. levels

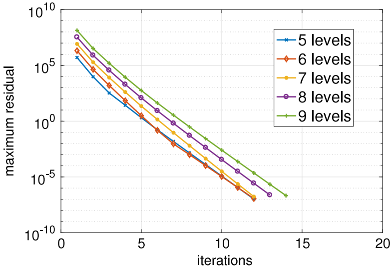

History of the convergence of the multigrid based on the fixed-stress split smoother for different numbers of refinement levels

Coupled flow and porous media problems

Free flow $\overset{interface}{\Longleftrightarrow}$ Flow in the porous medium

Coupled flow and porous media problems

Free flow $\overset{\textit{interface}}{\Longleftrightarrow}$ Flow in the porous medium

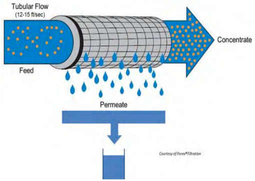

(a) filtration process

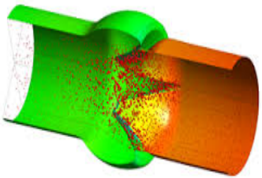

(b) blood flow simulation

(c) flooding simulation

(d) waste water treatment

Coupled flow and porous media problems

Free flow $\overset{\textit{interface}}{\Longleftrightarrow}$ Flow in the porous medium

DIFFERENT APPROACHES to solve the coupled problem:

- Domain Decomposition Methods:
  Decoupling the global problem so that mainly independent subproblems are to be solved.
- Monolithic Methods:
  Simultaneous solution of the coupled multi-physics system. Preconditioners and Multigrid methods.

Basic equations

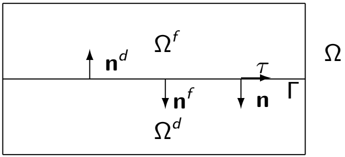

Figure: Geometry of the coupled Darcy/Stokes problem.

Porous medium description

$$
\begin{aligned}
\mathbb{K}^{-1}\mathbf{u}^d + \nabla p^d = \mathbf{0} \quad & \text{in } \Omega^d \,, \\
\nabla \cdot \mathbf{u}^d = f^d \quad & \text{in } \Omega^d \,.
\end{aligned}
$$

- $\mathbf{u}^d = (u^d, v^d)$ and p^d.
- The hydraulic conductivity tensor $\mathbb{K} = K\mathbb{I}$, $K > 0$.

Free flow description:

$$
\begin{aligned}
-\nabla \cdot \boldsymbol{\sigma}^f = \mathbf{f}^f \quad & \text{in } \Omega^f \,, \\
\nabla \cdot \mathbf{u}^f = 0 \quad & \text{in } \Omega^f \,.
\end{aligned}
$$

- $\mathbf{u}^f = (u^f, v^f)$ and p^f.
- $\boldsymbol{\sigma}^f = -p^f \mathbf{I} + 2\nu \mathbf{D}(\mathbf{u}^f)$, $\mathbf{D}(\mathbf{u}^f) = (\nabla \mathbf{u}^f + (\nabla \mathbf{u}^f)^T)/2$.

Interface conditions

We fix the normal vector to the interface to be $\mathbf{n} = \mathbf{n}^f = -\mathbf{n}^d$ and we denote $\boldsymbol{\tau}$ as the tangential unit vector at the interface Γ.

- Mass conservation:
$$\mathbf{u}^f \cdot \mathbf{n} = \mathbf{u}^d \cdot \mathbf{n} \quad \text{on } \Gamma \, .$$
- Balance of normal stresses:
$$-\mathbf{n} \cdot \boldsymbol{\sigma}^f \cdot \mathbf{n} = p^d \quad \text{on } \Gamma.$$
- Beavers-Joseph-Saffman condition: (α is a parameter)
$$\alpha \mathbf{u}^f \cdot \boldsymbol{\tau} + \boldsymbol{\tau} \cdot \boldsymbol{\sigma}^f \cdot \mathbf{n} = 0 \quad \text{on } \Gamma \, ,$$

  No-slip condition:
$$\mathbf{u}^f \cdot \boldsymbol{\tau} = 0 \quad \text{on } \Gamma \, .$$

Staggered grids

The computational domain is partitioned into square blocks of size $h \times h$, so that the grid is conforming at the interface Γ

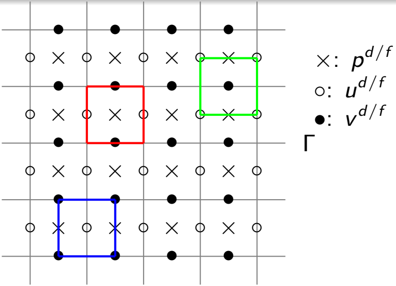

Figure: Staggered grid location of unknowns for the coupled model, and corresponding control volumes.

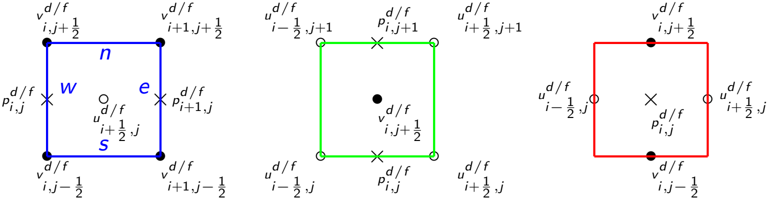

Figure: Control volumes for $u^{d/f}$ (left), $v^{d/f}$ (middle), $p^{d/f}$ (right).

Discretization at the interface

A special discretization at and near the points on the interface
(combining the approximation of the governing equations and the considered interface conditions)

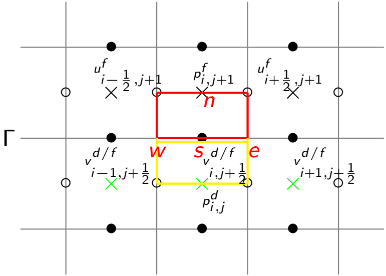

Figure: Staggered grid location of the unknowns for the interface conditions.

$$-\frac{(\sigma_{xy})_e-(\sigma_{xy})_w}{h}-\frac{(\sigma_{yy})_n-(\sigma_{yy})_s}{h/2}=(f_2^f)_{i,j+\frac{1}{2}}$$

- $(\sigma_{yy})_n$
- $(\sigma_{yy})_s = -p^d_s$
- $(\sigma_{xy})_e$ and $(\sigma_{xy})_w$

Beavers-Joseph-Saffman condition:

$$\alpha u^f_e - \nu\left(\frac{u^f_{i+\frac{1}{2},j+1}-u^f_e}{h/2}+\frac{v^f_{i+1,j+\frac{1}{2}}-v^f_{i,j+\frac{1}{2}}}{h}\right)=0$$

Peiyao Luo, Carmen Rodrigo, Francisco J. Gaspar, Cornelis W. Oosterlee, *Uzawa smoother in multigrid for the coupled Porous Medium and Stokes Flow System*, *SIAM Journal on Scientific Computing*, 2017.

Saddle point system

$$\begin{pmatrix} A & B^T \\ B & 0 \end{pmatrix} \begin{pmatrix} \mathbf{u} \\ p \end{pmatrix} = \begin{pmatrix} \mathbf{g} \\ f \end{pmatrix}$$

- B^T: discrete gradient. B: minus discrete divergence.
- A: discrete $-\nu\Delta$ for the Stokes equation.
  discrete $K^{-1}I$ for the Darcy equation.

Coupled system

$$\begin{pmatrix} A^d & 0 & (B^d)^T & 0 \\ 0 & A^f & R & (B^f)^T \\ B^d & R & 0 & 0 \\ 0 & B^f & 0 & 0 \end{pmatrix} \begin{pmatrix} \mathbf{u}^d \\ \mathbf{u}^f \\ p^d \\ p^f \end{pmatrix} = \begin{pmatrix} \mathbf{0} \\ \mathbf{f}^f \\ f^d \\ 0 \end{pmatrix},$$

$$A = \begin{pmatrix} A^d & 0 \\ 0 & A^f \end{pmatrix}, \quad B = \begin{pmatrix} B^d & R \\ 0 & B^f \end{pmatrix}, \quad B^T = \begin{pmatrix} (B^d)^T & 0 \\ R & (B^f)^T \end{pmatrix},$$

where R contains the relations given by the interface discretization

Multigrid for the coupled problem

Multigrid components:

- Choice of coarse grids and operators:
  - Standard coarsening
  - Γ is present on the complete grid hierarchy
  - Direct discretization of the continuous operators on coarse grids

Multigrid for the coupled problem

Multigrid components:

- Choice of coarse grids and operators:
  - Standard coarsening
  - Γ is present on the complete grid hierarchy
  - Direct discretization of the continuous operators on coarse grids
- Inter-grid transfer operators:
  - take into account the staggered arrangement of the unknowns

$$I_{h,2h}^{u} = \frac{1}{8}\begin{pmatrix} 1 & 2 & 1 \\ & * & \\ 1 & 2 & 1 \end{pmatrix}_h, \quad I_{h,2h}^{v} = \frac{1}{8}\begin{pmatrix} 1 & & 1 \\ 2 & * & 2 \\ 1 & & 1 \end{pmatrix}_h, \quad I_{h,2h}^{p} = \frac{1}{4}\begin{pmatrix} 1 & & 1 \\ & * & \\ 1 & & 1 \end{pmatrix}_h$$

  - Prolongation operators: the adjoints of the restrictions.
  - Inter-grid operators must be accordingly altered at boundary points and at the interface points

Multigrid for the coupled problem

Multigrid components:

- Choice of coarse grids and operators:
  - Standard coarsening
  - Γ is present on the complete grid hierarchy
  - Direct discretization of the continuous operators on coarse grids
- Inter-grid transfer operators:
  - take into account the staggered arrangement of the unknowns

$$I_{h,2h}^{u} = \frac{1}{8}\begin{pmatrix} 1 & 2 & 1 \\ & * & \\ 1 & 2 & 1 \end{pmatrix}_h, \quad I_{h,2h}^{v} = \frac{1}{8}\begin{pmatrix} 1 & & 1 \\ 2 & * & 2 \\ 1 & & 1 \end{pmatrix}_h, \quad I_{h,2h}^{p} = \frac{1}{4}\begin{pmatrix} 1 & & 1 \\ & * & \\ 1 & & 1 \end{pmatrix}_h$$

  - Prolongation operators: the adjoints of the restrictions.
  - Inter-grid operators must be accordingly altered at boundary points and at the interface points
- Type of cycle: comparison of $V-$ and $W-$cycles

Multigrid for the coupled problem

Multigrid components:

- Choice of coarse grids and operators:
  - Standard coarsening
  - Γ is present on the complete grid hierarchy
  - Direct discretization of the continuous operators on coarse grids
- Inter-grid transfer operators:
  - take into account the staggered arrangement of the unknowns

$$I^u_{h,2h} = \frac{1}{8}\begin{pmatrix} 1 & 2 & 1 \\ & * & \\ 1 & 2 & 1 \end{pmatrix}_h, \quad I^v_{h,2h} = \frac{1}{8}\begin{pmatrix} 1 & & 1 \\ 2 & * & 2 \\ 1 & & 1 \end{pmatrix}_h, \quad I^p_{h,2h} = \frac{1}{4}\begin{pmatrix} 1 & & 1 \\ & * & \\ 1 & & 1 \end{pmatrix}_h$$

  - Prolongation operators: the adjoints of the restrictions.
  - Inter-grid operators must be accordingly altered at boundary points and at the interface points
- Type of cycle: comparison of $V-$ and $W-$cycles
- Smoother???

Uzawa smoother

$$\begin{pmatrix} A & B^T \\ B & 0 \end{pmatrix} = \begin{pmatrix} M_A & \\ B & -\omega^{-1} I \end{pmatrix} - \begin{pmatrix} M_A - A & -B^T \\ & -\omega^{-1} I \end{pmatrix},$$

- ω: some positive parameter.
- M_A: Symmetric Gauss-Seidel for velocities

$$M_A = (D_A + L_A) D_A^{-1} (D_A + U_A)$$

The decoupled iteration can be described as:

$$\begin{pmatrix} M_A & \\ B & -\omega^{-1} I \end{pmatrix} \begin{pmatrix} \widehat{\mathbf{u}} \\ \widehat{p} \end{pmatrix} = \begin{pmatrix} M_A - A & -B^T \\ & -\omega^{-1} I \end{pmatrix} \begin{pmatrix} \mathbf{u} \\ p \end{pmatrix} + \begin{pmatrix} \mathbf{g} \\ f \end{pmatrix}$$

- apply smoother M_A to relax the system $A\mathbf{u} = \mathbf{g} - B^T p$;
  i.e., $\hat{\mathbf{u}} = \mathbf{u} + M_A^{-1} \left(\mathbf{g} - A\mathbf{u} - B^T p \right)$;
- update the pressure: $\hat{p} = p + \omega (B\hat{\mathbf{u}} - f)$.
- Optimal Parameter ω_{opt}?

Comparison between LFA and asymptotic results

- Darcy: $\omega_{opt} = \dfrac{h^2}{5K}$
- Stokes: $\omega_{opt} = \nu$

	Darcy		Stokes	
$\nu_1 + \nu_2$	$K = 1$	$K = 10^{-6}$	$\nu = 1$	$\nu = 10^{-6}$
2	0.600	0.600	0.304	0.304
3	0.360	0.360	0.143	0.143
4	0.216	0.216	0.081	0.081

Table: Two-grid convergence factors, ρ predicted by LFA.

	K	1		10^{-6}	
	ν	1	10^{-6}	1	10^{-6}
$\nu_1 + \nu_2$	2	0.59	0.59	0.59	0.59
	3	0.36	0.36	0.36	0.36
	4	0.21	0.21	0.21	0.21

Table: Asymptotic convergence factors, ρ_h, for the coupled problem.

Multiblock multigrid algorithm

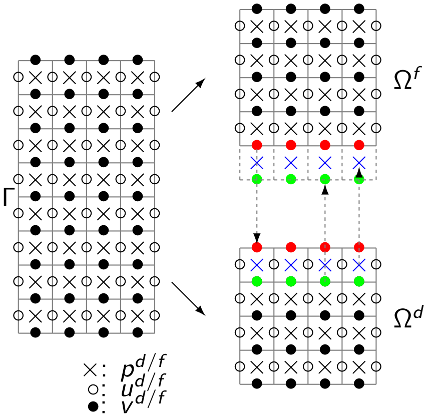

Multiblock two-grid algorithm: (with only pre-smoothing)

1. Relax velocity unknowns.
2. *Stokes to Darcy*: $v^f \to v^d$ (●).
3. Update pressure unknowns.
4. *Darcy to Stokes*: $p^d \to p^f$ (×).
5. Compute the residual.
6. *Darcy to Stokes*: $r^d \to r^f$ (●).
7. Restrict the residual.
8. Solve exactly the defect equation on the coarsest grid.
9. *Stokes to Darcy*: $e^f \to e^d$.
10. Interpolation and correction.

Beavers-Joseph-Saffman interface condition

Analytical solution

$$\mathbf{u}^d(x,y) = \begin{pmatrix} u^d(x,y) \\ v^d(x,y) \end{pmatrix} = \begin{pmatrix} -Ke^y \cos x \\ -Ke^y \sin x \end{pmatrix},$$

$$p^d(x,y) = e^y \sin x,$$

$$\mathbf{u}^f(x,y) = \begin{pmatrix} u^f(x,y) \\ v^f(x,y) \end{pmatrix} = \begin{pmatrix} \lambda'(y) \cos x \\ \lambda(y) \sin x \end{pmatrix},$$

$$p^f(x,y) = 0,$$

where $\lambda(y) = -K - \frac{g\,y}{2\nu} + (-\frac{\alpha}{4\nu^2} + \frac{K}{2})y^2.$

- $\Omega = (0,1) \times (-1,1)$, $\Omega^d = (0,1) \times (-1,0)$, $\Omega^f = (0,1) \times (0,1)$.
- Interface $\Gamma = (0,1) \times \{0\}$.
- Free flow: Dirichlet conditions for u^f and v^f at the outer boundaries.
- Porous medium: fixed p^d at the bottom, Dirichlet conditions for u^d and v^d at the lateral walls.

Beavers-Joseph-Saffman interface condition

	64×128	128×256	256×512
u^d	1.42×10^{-5}	3.63×10^{-6}	9.19×10^{-7}
v^d	4.09×10^{-5}	1.19×10^{-5}	3.38×10^{-6}
p^d	9.11×10^{-6}	2.32×10^{-6}	5.84×10^{-7}
u^f	1.21×10^{-5}	3.06×10^{-6}	7.71×10^{-7}
v^f	2.97×10^{-5}	7.66×10^{-6}	1.95×10^{-6}
p^f	4.74×10^{-3}	2.38×10^{-3}	1.19×10^{-3}

Table: Maximum norm errors of variables $u^{d/f}$, $v^{d/f}$, $p^{d/f}$ for different grid-sizes, by considering fixed values $\nu = 1$ and $K = 1$, and prescribing the Beavers-Joseph-Saffman condition at the interface with $\alpha = 1$.

Beavers-Joseph-Saffman interface condition

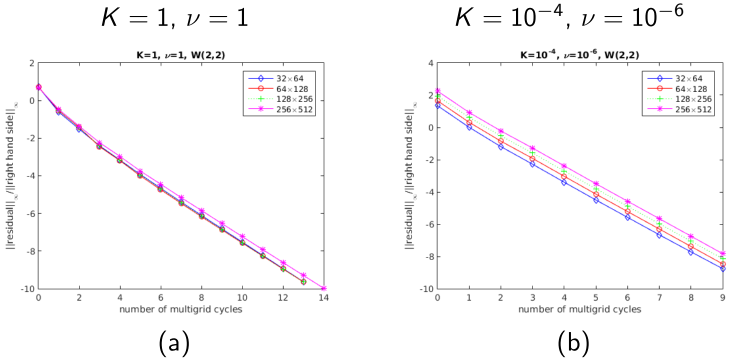

Figure: History of the convergence of the $W(2,2)-$multigrid method for different values of the physical parameters.

Realistic problem: cross-flow membrane filtration model

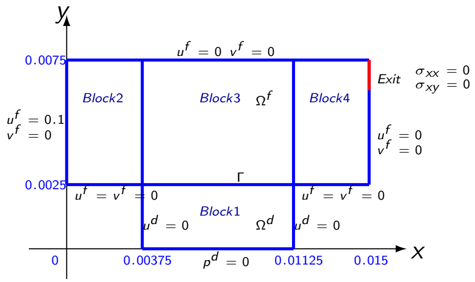

Figure: Geometry of the coupled problem.

- 4 blocks, $K = 0.1$ or $K = 10^{-6}$, $\nu = 10^{-6}$.
- Beavers-Joseph-Saffman interface condition.
- Communications on each level.
- Excellent multigrid convergence factor 0.2 for $W(2,2)$-cycle for the coupled system.

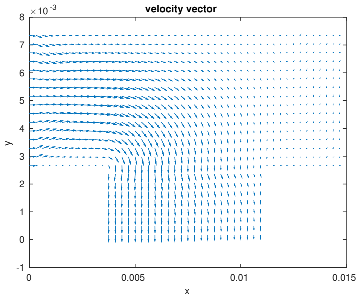

(a) $K = 0.1$

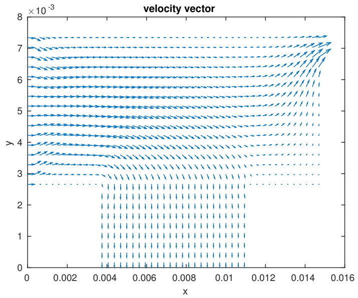

(b) $K = 10^{-6}$

Figure: Velocity vectors over the cross-flow filtration domain with different values of permeability.

Heterogeneity test

To simulate heterogeneity in the porous medium, a Gaussian model characterized by parameters λ_g and σ_g^2 is considered, i.e.,

$$C(d_g) = \sigma_g^2 \exp\left(-\frac{d_g^2}{\lambda_g}\right) ,$$

where d_g is the distance between two points, λ_g defines the correlation length and σ_g^2 represents the variance.

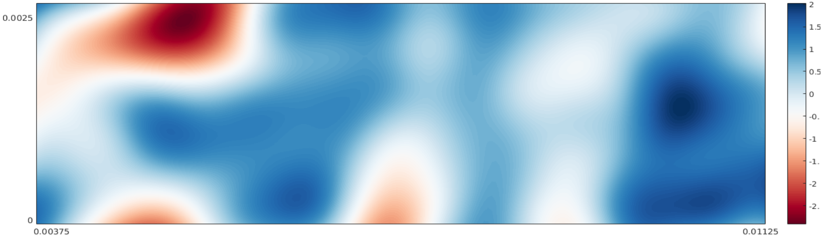

Figure: Example of random field of hydraulic conductivity K in log-scale, with parameters $\lambda_g = 0.3$ and $\sigma_g^2 = 1$.

Heterogeneity test

- Two different values for parameter λ_g: $\lambda_g = 0.1$ denotes a more heterogeneous porous medium than $\lambda_g = 0.3$.
- 50 realizations of the random field are generated and we record the multigrid convergence factors of the $W(2,2)$-cycle.

h^{-1}	$\lambda_g = 0.3$	$\lambda_g = 0.1$
25600	0.19	0.20
12800	0.19	0.21
6400	0.20	0.29

Table: Mean value of the multigrid convergence factors after 50 realizations.

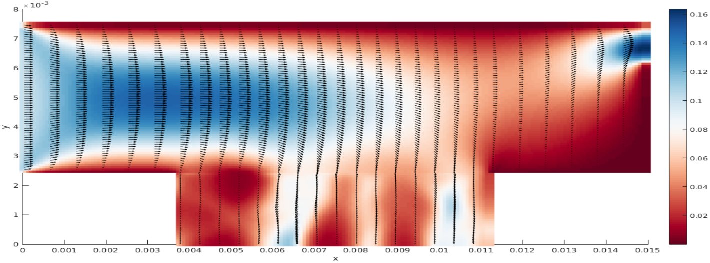

Figure: L_2 norm of the velocity vectors over the cross flow filtration domain.

Coupled Stokes and Deformable Porous Medium System

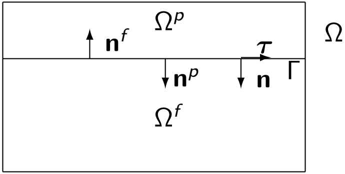

Deformable Porous Media

$$-\nabla \cdot \boldsymbol{\sigma}^p = \mathbf{f}^p \quad \text{in } \Omega^p$$

$$\frac{\partial}{\partial t}(\nabla \cdot \mathbf{u}^p) + \nabla \cdot \mathbf{q}^p = f^p \quad \text{in } \Omega^p$$

$$\mathbf{q}^p = -K \nabla p^p \quad \text{in } \Omega^p$$

- $\mathbf{u}^p = (u^p, v^p)$ and p^p
- $\boldsymbol{\sigma}^p = \boldsymbol{\sigma}^E - p^p \mathbf{I}$
- $\boldsymbol{\sigma}^E(\mathbf{u}^p) = 2\mu \mathbf{D}(\mathbf{u}^p) + \lambda tr(\mathbf{D}(\mathbf{u}^p))\mathbf{I}$

Stokes Flow

$$\rho \frac{\partial \mathbf{u}^f}{\partial t} - \nabla \cdot \boldsymbol{\sigma}^f = \mathbf{f}^f \quad \text{in } \Omega^f$$

$$\nabla \cdot \mathbf{u}^f = 0 \quad \text{in } \Omega^f$$

- $\mathbf{u}^f = (u^f, v^f)$ and p^f
- $\boldsymbol{\sigma}^f = -p^f \mathbf{I} + 2\nu \mathbf{D}(\mathbf{u}^f)$
- $\mathbf{D}(\mathbf{u}^f) = (\nabla \mathbf{u}^f + (\nabla \mathbf{u}^f)^T)/2$

Interface conditions

- Mass conservation:

$$(\mathbf{u}^f - \frac{\partial \mathbf{u}^p}{\partial t}) \cdot \mathbf{n} = \mathbf{q}^p \cdot \mathbf{n} \ ,$$

- Balance of normal stresses in the fluid phase:

$$\mathbf{n} \cdot \boldsymbol{\sigma}^f \mathbf{n} = -p^p$$

- Conservation of momentum:

$$\mathbf{n} \cdot \boldsymbol{\sigma}^f \mathbf{n} - \mathbf{n} \cdot \boldsymbol{\sigma}^p \mathbf{n} = 0$$

and

$$\boldsymbol{\tau} \cdot \boldsymbol{\sigma}^f \mathbf{n} - \boldsymbol{\tau} \cdot \boldsymbol{\sigma}^p \mathbf{n} = 0$$

- Beavers-Joseph-Saffman interface condition:

$$-\boldsymbol{\tau} \cdot \boldsymbol{\sigma}^f \mathbf{n} = \beta(\mathbf{u}^f - \frac{\partial \mathbf{u}^p}{\partial t}) \cdot \boldsymbol{\tau}$$

- No-slip condition:

$$\mathbf{u}^f \cdot \boldsymbol{\tau} = \frac{\partial \mathbf{u}^p}{\partial t} \cdot \boldsymbol{\tau}$$

Saddle point structure

At each time step: $\begin{pmatrix} A & B^T \\ B & -C \end{pmatrix} \begin{pmatrix} \mathbf{u} \\ p \end{pmatrix} = \begin{pmatrix} \mathbf{g} \\ f \end{pmatrix}$

- B^T and $B \equiv$ discrete gradient and the negative discrete divergence
- For the poroelastic system:
  - A is $-\mu\Delta - \nabla(\lambda+\mu)\nabla\cdot$ and C corresponds to $-\tau\nabla\cdot(K\nabla p)$
- For the Stokes system:
  - A represents $\dfrac{\rho}{\tau}I - \nu\Delta$ and C is a zero block

$$\begin{pmatrix} A^f & R^T & (B^f)^T & (R')^T \\ R & A^p & 0 & (B^p)^T \\ B^f & 0 & 0 & 0 \\ R' & B^p & 0 & -C^p \end{pmatrix} \begin{pmatrix} \mathbf{u}^f \\ \mathbf{u}^p \\ p^f \\ p^p \end{pmatrix} = \begin{pmatrix} \mathbf{f}^f \\ \mathbf{f}^p \\ 0 \\ f^p \end{pmatrix}$$

$$A = \begin{pmatrix} A^f & R^T \\ R & A^p \end{pmatrix}, B = \begin{pmatrix} B^f & 0 \\ R' & B^p \end{pmatrix}, -C = \begin{pmatrix} 0 & 0 \\ 0 & -C^p \end{pmatrix},$$

wheere R and R' contain the coupling at and near the interface.

Monolithic multigrid

- Uzawa smoother
- Optimal relaxation parameter
  - Poroelasticity system:

$$\omega^p = \frac{h^2(\lambda + 2\mu)}{5K\tau(\lambda + 2\mu) + h^2}$$

  - Stokes system:

$$\omega^f = \nu + \frac{\rho h^2}{8\tau}$$

Relaxation parameters do not only depend on the model coefficients but also on the grid size and on time step τ, thus ω^p and ω^f are different on each grid of the hierarchy in the multigrid method

Analytical test. No-slip condition

Analytical solution

$$
\begin{aligned}
u^f &= u^p = (y^2 - y)e^t \\
v^f &= v^p = 0 \\
p^f &= p^p = xe^t
\end{aligned}
$$

- $\Omega = (0,1) \times (0,2)$, $\Omega^f = (0,1) \times (0,1)$, $\Omega^p = (0,1) \times (1,2)$
- Interface $\Gamma = (0,1) \times \{1\}$
- Dirichlet boundary conditions for displacements and pressure at the lateral boundaries of Ω^p.
- Stress conditions at the top of Ω^p, where the fluid pressure is fixed
- In Ω^f, stress conditions at both inlet and outlet, while a symmetric boundary condition is imposed at the bottom.
- Interface conditions with the simplified no-slip interface condition

Analytical test. No-slip condition

	$64 \times 128 \times 4$	$128 \times 256 \times 8$	$256 \times 512 \times 16$
u^f	2.01×10^{-4}	9.73×10^{-5}	4.76×10^{-5}
v^f	1.20×10^{-4}	4.47×10^{-5}	2.31×10^{-5}
p^f	3.16×10^{-3}	1.63×10^{-3}	7.95×10^{-4}
u^p	6.77×10^{-3}	3.46×10^{-3}	1.75×10^{-3}
v^p	6.38×10^{-4}	3.26×10^{-4}	1.65×10^{-4}
p^p	3.87×10^{-3}	1.68×10^{-3}	7.75×10^{-4}

Table: Maximum norm errors of variables $u^{f/p}$, $v^{f/p}$ and $p^{f/p}$ for different grid sizes with parameters $K = 1$, $\lambda = 1$, $\mu = 1$, $\nu = 1$ and $\rho = 1$.

Analytical test. No-slip condition

$K = 10^{-4}$, $\nu = 10^{-3}$ $\qquad$ $K = 10^{-6}$, $\nu = 10^{-6}$

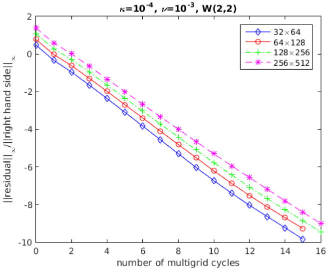

(a)

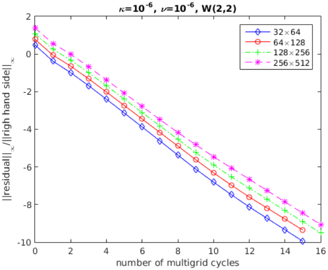

(b)

Figure: History of the convergence of the $W(2,2)-$multigrid method for different values of the physical parameters

Multi-block realistic test

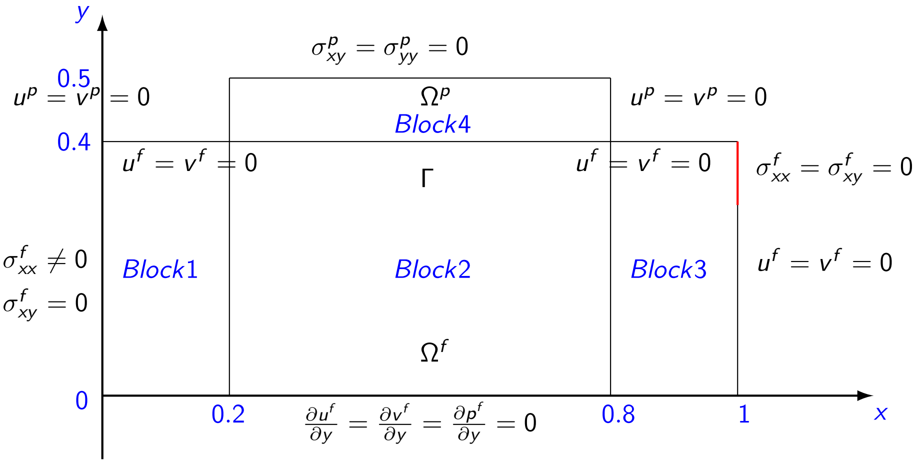

- Fluid inflow in Ω^f: $\sigma^f_{xx} = -20000$
- Small exit at the right vertical boundary (stress-free boundary)
- $K = 10^{-4}$, $\lambda = 10^6$, $\mu = 2.5 \times 10^5$, $\nu = 0.0035$ and $\rho = 1$.

- Drained conditions ($p^p = 0$) for pressure on the exterior of Ω^p

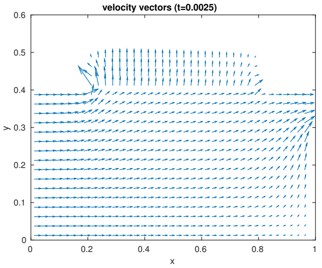

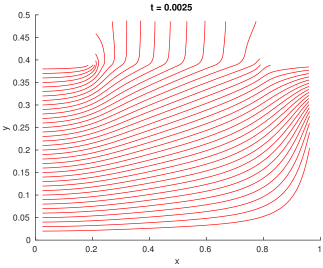

- Impermeable conditions on the exterior of Ω^p

$K = 0.01$

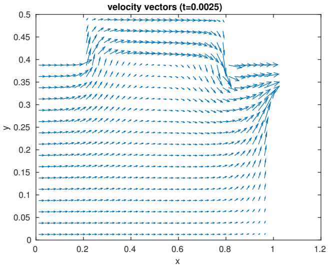

$K = 10^{-4}$

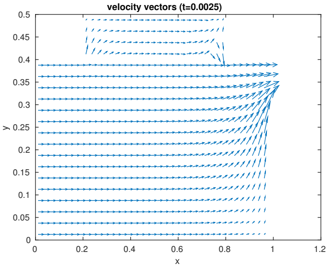

Flow in fractured porous media

blogs.agu.org

Outcrop in the Sotra island (Flemisch et al. 2018)

APPLICATIONS

- Petroleum extraction
- Long-term CO_2 and nuclear waste storage
- Geothermal energy production
- Biomedical applications, e.g., where capillaries can be treated as fractures in the matrix

Flow in fractured porous media

blogs.agu.org

Outcrop in the Sotra island (Flemisch et al. 2018)

APPLICATIONS

- Petroleum extraction
- Long-term CO_2 and nuclear waste storage
- Geothermal energy production
- Biomedical applications, e.g., where capillaries can be treated as fractures in the matrix

- Development of numerical schemes to discretize fracture models
- Design of efficient solvers for the corresponding flow models

Flow in fractured porous media

blogs.agu.org

Outcrop in the Sotra island (Flemisch et al. 2018)

APPLICATIONS

- Petroleum extraction
- Long-term CO_2 and nuclear waste storage
- Geothermal energy production
- Biomedical applications, e.g., where capillaries can be treated as fractures in the matrix

- Development of numerical schemes to discretize fracture models
- Design of efficient solvers for the corresponding flow models

Models for flow in fractured media

Fractures can be incorporated to flow models in essentially two ways:

- At small scales: DUAL-POROSITY MODELS
  - Specific locations of micro-fractures are difficult to determine
  - The fractures' network and the bulk or porous matrix are two interacting continua related by a transfer function
- At large scales: DISCRETE FRACTURE MODELS (DFM)
  - Localized networks of faults and macro-fractures
  - Fractures can behave either as preferential flow paths or as geological barriers

Models for flow in fractured media

Fractures can be incorporated to flow models in essentially two ways:

- At small scales: DUAL-POROSITY MODELS
  - Specific locations of micro-fractures are difficult to determine
  - The fractures' network and the bulk or porous matrix are two interacting continua related by a transfer function

- At large scales: DISCRETE FRACTURE MODELS (DFM)
  - Localized networks of faults and macro-fractures
  - Fractures can behave either as preferential flow paths or as geological barriers

The mixed-dimensional model

- Fine meshing of the fracture domain to guarantee accurate approximations.
- The thickness of the fractures is very small compared to their length and also compared to the typical size of the domain of interest.

The mixed-dimensional model

- Fine meshing of the fracture domain to guarantee accurate approximations.
- The thickness of the fractures is very small compared to their length and also compared to the typical size of the domain of interest.

A reduced model (or mixed-dimensional model) can be considered in which the fractures are treated as $(n-1)$ dimensional interfaces in an n dimensional medium

- Different models can be considered within the fractures and in the porous matrix.
- Here: single-phase Darcy-Darcy and Darcy-Fochheimer couplings between the fractures and the porous matrix.

The mixed-dimensional model

- For simplicity, we assume the existence of a single fracture Ω_f that separates Ω into two connected subdomains: Ω_1, Ω_2.

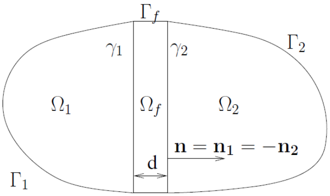

Transmission problem

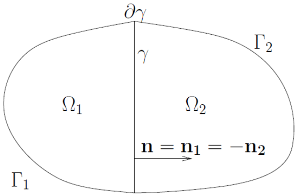

Interface problem

V. Martin, J. Jaffré, J.E. Roberts (2005) Modeling fractures and barriers as interfaces for flow in porous media, SIAM J. Sci. Comp. 26, pp. 1667-1691.

The mixed-dimensional model problem. Darcy-Darcy

- Consider linear Darcy flow in the subdomains

$$\mathbf{u}_i = -K_i \nabla p_i, \quad \operatorname{div} \mathbf{u}_i = q_i, \quad \text{in } \Omega_i, \text{ for } i = 1, 2,$$

with $p_i = 0$ on $\partial\Omega_i$, for $i = 1, 2$. We assume K_i is diagonal.

- Consider linear Darcy flow in the fracture too

$$\mathbf{u}_\gamma = -K_{f,\tau}\, d\, \nabla_\tau p_\gamma, \quad \operatorname{div}_\tau \mathbf{u}_\gamma = q_\gamma + (\mathbf{u}_1 \cdot \mathbf{n}_1 + \mathbf{u}_2 \cdot \mathbf{n}_2), \quad \text{on } \gamma,$$

with $p_\gamma = 0$ on $\partial\gamma$.

- Impose the interface condition

$$\alpha_\gamma\, p_i = \alpha_\gamma\, p_\gamma + (\xi\, \mathbf{u}_i \cdot \mathbf{n}_i - (1-\xi)\, \mathbf{u}_{i+1} \cdot \mathbf{n}_{i+1}), \qquad \text{in } \gamma, \text{ for } i = 1, 2,$$

where $\alpha_\gamma = \frac{2K_{f,n}}{d}$, $\xi \in \left(\frac{1}{2}, 1\right]$, and $i + 1 = 1$ if $i = 2$.

The weak formulation

We consider the following function spaces

$$M = L^2(\Omega_1) \times L^2(\Omega_2) \times L^2(\gamma),$$

$$\mathbf{W} = \{\mathbf{u} = (\mathbf{u}_1, \mathbf{u}_2, \mathbf{u}_\gamma) \in H(\mathrm{div}, \Omega_1) \times H(\mathrm{div}, \Omega_2) \times H(\mathrm{div}_\tau, \gamma) : \mathbf{u}_i \cdot \mathbf{n}_i \in L^2(\gamma), i = 1, 2\}.$$

- Define the forms $a : \mathbf{W} \times \mathbf{W} \to \mathbb{R}$ and $b : \mathbf{W} \times M \to \mathbb{R}$ by

$$a(\mathbf{u}, \mathbf{v}) = \sum_{i=1}^{2} \left(\mathbf{K}_i^{-1}\mathbf{u}_i, \mathbf{v}_i\right)_{\Omega_i} + \left((d\, K_{f,\tau})^{-1}\, \mathbf{u}_\gamma, \mathbf{v}_\gamma\right)_\gamma + \sum_{i=1}^{2} \left(\alpha_\gamma^{-1}(\xi\, \mathbf{u}_i \cdot \mathbf{n}_i - (1-\xi)\, \mathbf{u}_{i+1} \cdot \mathbf{n}_{i+1}), \mathbf{v}_i \cdot \mathbf{n}_i\right)_\gamma,$$

$$b(\mathbf{u}, r) = \sum_{i=1}^{2} (\mathrm{div}\, \mathbf{u}_i, r_i)_{\Omega_i} + (\mathrm{div}_\tau\, \mathbf{u}_\gamma, r_\gamma)_\gamma - \left(\sum_{i=1}^{2} \mathbf{u}_i \cdot \mathbf{n}_i, r_\gamma\right)_\gamma .$$

- Define the linear form $L_q : M \to \mathbb{R}$ by:

$$L_q(r) = \sum_{i=1}^{2} (q_i, r_i)_{\Omega_i} + (q_\gamma, r_\gamma)_\gamma .$$

The weak formulation

- The variational problem may be written in standard mixed form as:

Find $\mathbf{u} = (\mathbf{u}_1, \mathbf{u}_2, \mathbf{u}_\gamma) \in \mathbf{W}$, $p = (p_1, p_2, p_\gamma) \in M$ s.t. :

$$\begin{cases} a(\mathbf{u}, \mathbf{v}) - b(\mathbf{v}, p) = 0 & \forall \, \mathbf{v} \in \mathbf{W}, \\ b(\mathbf{u}, r) = L_q(r) & \forall \, r \in M. \end{cases}$$

V. Martin, J. Jaffré, J.E. Roberts (2005) Modeling fractures and barriers as interfaces for flow in porous media, SIAM J. Sci. Comp. 26, pp. 1667-1691.

The mixed finite element method

- Let $\mathcal{T}_{h,i}$ be a rectangular partition of Ω_i, $i = 1, 2$ and suppose that the meshes $\mathcal{T}_{h,i}$ match at the interface γ, i.e. they induce a unique partition on γ denoted by $\mathcal{T}_{h,\gamma}$.

- Then, $\mathcal{T}_h = \cup \mathcal{T}_{h,i}$, $i = 1, 2, \gamma$, consists of both n dimensional elements in Ω_i and $(n-1)$-dimensional elements on γ.
- Let $\mathbf{W}_{h,i} \times M_{h,i}$ be the Raviart-Thomas mixed finite element spaces of lowest order associated with $\mathcal{T}_{h,i}$, $i = 1, 2, \gamma$.
- Let us define

$$\mathbf{W}_h = \mathbf{W}_{h,1} \oplus \mathbf{W}_{h,2} \oplus \mathbf{W}_{h,\gamma},$$

$$M_h = M_{h,1} \oplus M_{h,2} \oplus M_{h,\gamma}.$$

A quadrature rule

- For $\mathbf{v}, \mathbf{q} \in \mathbb{R}^2$, let us introduce the quadrature rule:

$$(\mathbf{v}, \mathbf{q})_{\mathbf{TM}} = (v_1, q_1)_{\mathbf{T}\times\mathbf{M}} + (v_2, q_2)_{\mathbf{M}\times\mathbf{T}}$$

  where the trapezoidal rule in one direction is tensored with the midpoint rule in the other.

- Define the form

$$a_h(\mathbf{u}, \mathbf{v}) = \sum_{i=1}^{2} \left(\mathbf{K}_i^{-1} \mathbf{u}_i, \mathbf{v}_i \right)_{\Omega_i, \mathbf{TM}} + \left((d\, K_{f,\tau})^{-1} \mathbf{u}_\gamma, \mathbf{v}_\gamma \right)_{\gamma, \mathbf{T}}$$
$$+ \sum_{i=1}^{2} \left(\alpha_\gamma^{-1} (\xi\, \mathbf{u}_i \cdot \mathbf{n}_i - (1-\xi)\, \mathbf{u}_{i+1} \cdot \mathbf{n}_{i+1}), \mathbf{v}_i \cdot \mathbf{n}_i \right)_\gamma$$

T. F. Russell and M. F. Wheeler, Finite element and finite difference methods for continuous flows in porous media, in The Mathematics of Reservoir Simulation, R. E. Ewing, ed., vol. 1 of Frontiers in Applied Mathematics, SIAM, Philadelphia, 1983, pp. 35-106.

The mixed finite element approximation

- The mixed finite element approximation for the interface problem may be written as:

$$\text{Find } \mathbf{u}_h = (\mathbf{u}_{h,1}, \mathbf{u}_{h,2}, \mathbf{u}_{h,\gamma}) \in \mathbf{W}_h,\ p_h = (p_{h,1}, p_{h,2}, p_{h,\gamma}) \in M_h \text{ s.t. :}$$
$$\begin{cases} a_h(\mathbf{u}_h, \mathbf{v}_h) - b(\mathbf{v}_h, p_h) = 0 & \forall\, \mathbf{v}_h \in \mathbf{W}_h, \\ b(\mathbf{u}_h, r_h) = L_q(r_h) & \forall\, r_h \in M_h. \end{cases}$$

- This method is closely related to the two-point flux approximation (TPFA) method.

  R. Eymard, T. Galloüet, C. Guichard, R. Herbin, and R. Masson (2014) TP or not TP, that is the question, Comput. Geosci., 18 pp. 285-296.

The algebraic linear system

The corresponding algebraic linear system is a saddle-point problem of the form:

$$\begin{bmatrix} A_1 & C^T & 0 & B_1^T & 0 & F_1^T \\ C^T & A_2 & 0 & 0 & B_2^T & F_2^T \\ 0 & 0 & A_\gamma & 0 & 0 & B_\gamma^T \\ B_1 & 0 & 0 & 0 & 0 & 0 \\ 0 & B_2 & 0 & 0 & 0 & 0 \\ F_1 & F_2 & B_\gamma & 0 & 0 & 0 \end{bmatrix} \begin{bmatrix} U_1 \\ U_2 \\ U_\gamma \\ P_1 \\ P_2 \\ P_\gamma \end{bmatrix} = \begin{bmatrix} 0 \\ 0 \\ 0 \\ * \\ * \\ * \end{bmatrix}$$

where A_i, $i = 1, 2, \gamma$, are diagonal matrices.

The monolithic multigrid method

- We need a hierarchy of grids of various sizes.
- Perform direct discretization of the problem on each grid.
- Perform W(2,2)-cycles.
- The coarsest grid should be built taking into account the location of the fractures.

The monolithic multigrid method

- We need a hierarchy of grids of various sizes.
- Perform direct discretization of the problem on each grid.
- Perform W(2,2)-cycles.
- The coarsest grid should be built taking into account the location of the fractures.

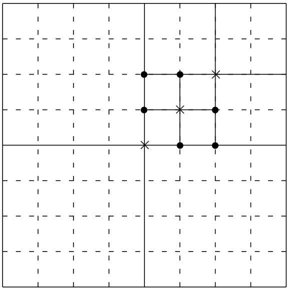

Coarsest grid corresponding to the fracture network for benchmark problem

The monolithic multigrid method

- We need a hierarchy of grids of various sizes.
- Perform direct discretization of the problem on each grid.
- Perform W(2,2)-cycles.
- The coarsest grid should be built taking into account the location of the fractures. Then, apply regular refinement on each cell of the initial mesh.

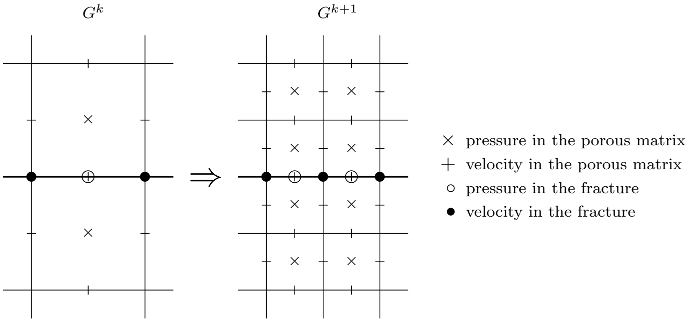

Grid refinement procedure and location of the unknowns

The KEY is to consider MIXED-DIMENSIONAL MULTIGRID COMPONENTS

MIXED-DIMENSIONAL INTER-GRID TRANSFER OPERATORS

- Inter-grid transfer operators in the porous matrix:

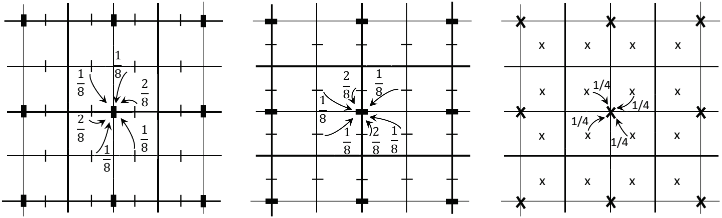

- Inter-grid transfer operators in the fracture:

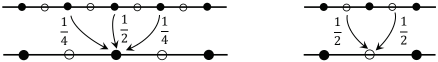

The monolithic multigrid method

The KEY is to consider MIXED-DIMENSIONAL MULTIGRID COMPONENTS

MIXED-DIMENSIONAL SMOOTHER

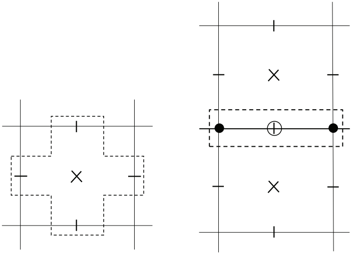

- × pressure in the porous matrix
- + velocity in the porous matrix
- ○ pressure in the fracture
- ● velocity in the fracture

- Use mixed-dimensional Vanka smoothers for the unknowns on the matrix and within the fractures.
- Consider block Gauss-Seidel smoother for the intersections (if any).

Example 1: one fracture with constant permeability

- Dirichlet boundary conditions for the fracture, width $d = 10^{-2}$.
- Permeability tensor in the fracture $\mathbf{K} = K_f\,\mathbf{Id}$.

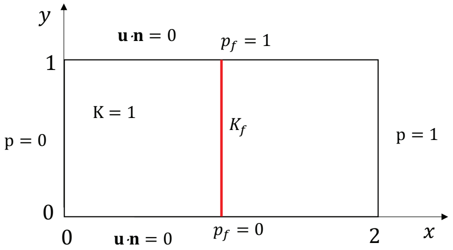

Example 1: one fracture with constant permeability

- Pressure distribution for $K_f = 10^2$ (left) and $K_f = 10^{-2}$ (right)

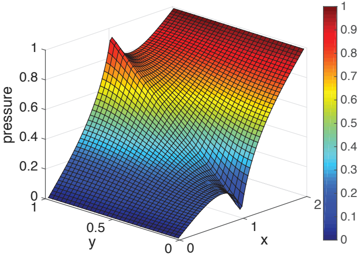

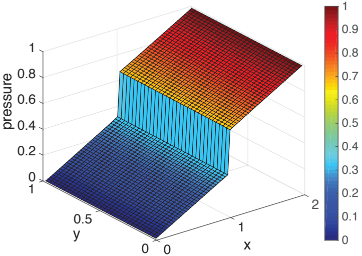

Example 1: one fracture with constant permeability

- Number of iterations to reduce the initial residual in a factor of 10^{-10} for different grid sizes and different values of K_f

	32×16	64×32	128×64	256×128	512×256
K_f	MG	MG	MG	MG	MG
10^{-6}	8	8	9	9	9
10^{-4}	8	8	9	9	9
10^{-2}	8	8	9	9	9
10^{2}	10	9	9	10	10
10^{4}	8	9	9	9	10
10^{6}	8	9	9	9	10

Example 1: one fracture with constant permeability

- Number of iterations to reduce the initial residual in a factor of 10^{-10} for different grid sizes and different values of K_f
  - as stand-alone solver (MG)
  - as preconditioner (Prec) of the Flexible GMRES method (a single $W(2,2)-$multigrid cycle per iteration)

	32×16	64×32	128×64	256×128	512×256
K_f	MG/Prec	MG/Prec	MG/Prec	MG/Prec	MG/Prec
10^{-6}	8/8	8/8	9/9	9/9	9/9
10^{-4}	8/8	8/8	9/9	9/9	9/9
10^{-2}	8/8	8/8	9/9	9/9	9/9
10^{2}	10/9	9/9	9/9	10/9	10/10
10^{4}	8/9	9/9	9/10	9/10	10/10
10^{6}	8/9	9/9	9/10	9/10	10/10

Example 1: one fracture with constant permeability

Heterogeneous porous medium

- The permeability in the porous matrix is represented by a lognormal random field. We consider the following Matérn covariance function,

$$C_\Phi(r) = \sigma_c^2 \frac{2^{1-\nu_c}}{\Gamma(\nu_c)} \left(2\sqrt{\nu_c}\frac{r}{\lambda_c}\right)^{\nu_c} K_\nu \left(2\sqrt{\nu_c}\frac{r}{\lambda_c}\right),$$

characterized by the set of parameters $\Phi = (\nu_c, \lambda_c, \sigma_c^2)$

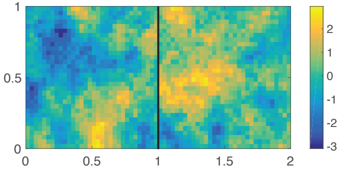

$\Phi_1 = (0.5, 0.3, 1)$

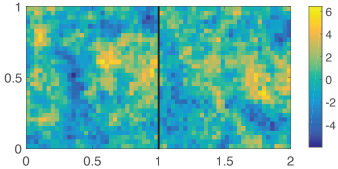

$\Phi_2 = (0.5, 0.1, 3)$

Average number of 9 iterations for the parameter set Φ_1, and around 13 iterations for Φ_2

Example 2: one fracture with variable permeability

- Neumann boundary conditions for the fracture, width $d = 10^{-2}$.
- Permeability tensor in the fracture:

$$\mathbf{K} = \begin{cases} K_{f1}\mathbf{Id}, & \text{if } 0 < y < \frac{1}{4} \text{ or } \frac{3}{4} < y < 1, \\ K_{f2}\mathbf{Id}, & \text{if } \frac{1}{4} < y < \frac{3}{4}. \end{cases}$$

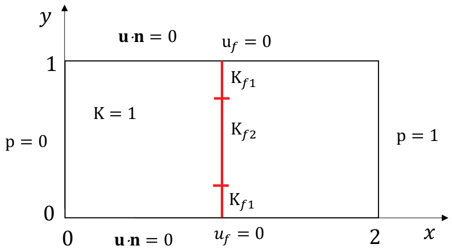

Example 2: one fracture with variable permeability

- Pressure distribution for $K_{f1} = 10^2$ and $K_{f2} = 2 \times 10^{-3}$ (left)
- Convergence of the multigrid method - residual vs. iterations (right)

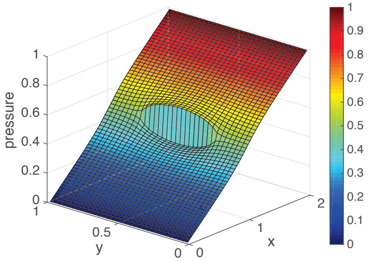

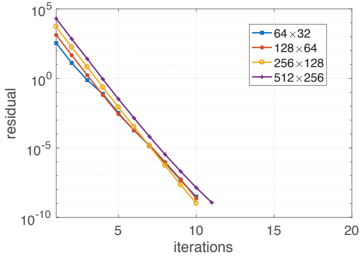

Example 3 : four fractures

- Fracture network and settings:

Setting 1 (S1)

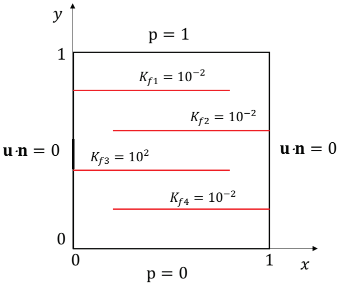

- Iterations to reduce the initial residual in a factor of 10^{-10}

	40×40	80×80	160×160	320×320	640×640	1280×1280
S1	9	9	10	10	11	11

Examples 3-4: four fractures

- Fracture network and settings:

Setting 1 (S1)

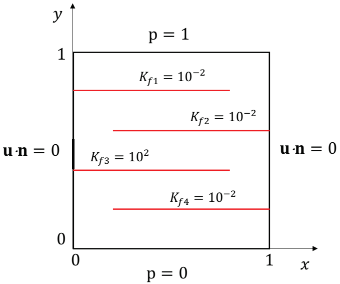

Setting 2 (S2)

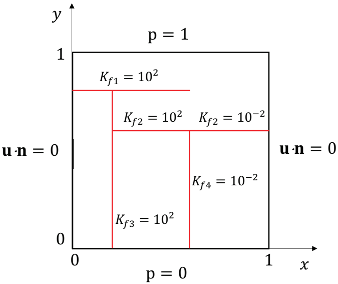

- Iterations to reduce the initial residual in a factor of 10^{-10}

	40×40	80×80	160×160	320×320	640×640	1280×1280
S1	9	9	10	10	11	11
S2	11	11	11	12	13	13

Example 5: benchmark problem

- Fracture network, width $d = 10^{-4}$.

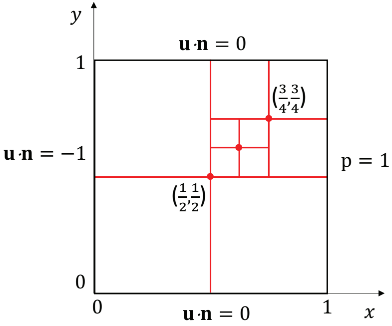

B. Flemisch, I. Berre, W. Boon, A. Fumagalli, N. Schwenck, A. Scotti, I. Stefansson, A. Tatomir (2018) Benchmarks for single-phase flow in fractured porous media, Adv. Water Resour. 111 pp. 239-258.

Example 5: benchmark problem

- Pressure distribution for $K_f = 10^4$ (left)
- Convergence of the multigrid method - residual vs. iterations (right)

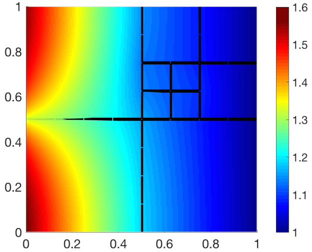

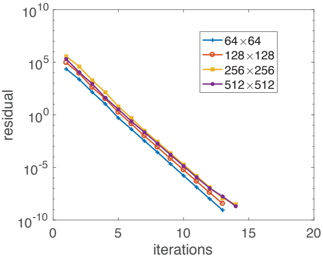

Example 5: benchmark problem

- Pressure distribution for $K_f = 10^{-4}$ (left)
- Convergence of the multigrid method - residual vs. iterations (right)

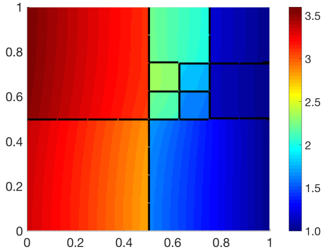

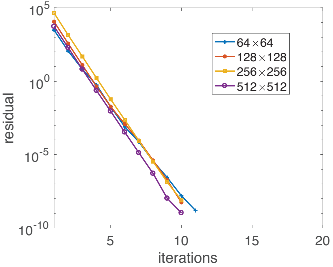

Example 6: Local Fourier analysis test

Local Fourier analysis (LFA) is the main quantitative analysis to predict the convergence rates of multigrid algorithms

- Comparison between the predicted LFA two-grid convergence factor for Darcy problem and the asymptotic convergence factors experimentally obtained from the numerical experiments performed in the fractured porous media.

LFA	One fracture		Four fractures		Benchmark
	Test 1	Test 2	Test 3	Test 4	
0.04	0.039	0.077	0.045	0.08	0.085

- Consider linear Darcy flow in the subdomains

$$\mathbf{u}_i = -K_i \nabla p_i, \quad \operatorname{div} \mathbf{u}_i = q_i, \quad \text{in } \Omega_i, \text{ for } i = 1, 2,$$

with $p_i = 0$ on $\partial\Omega_i$, for $i = 1, 2$. We assume K_i is diagonal.

- Consider nonlinear Darcy–Forchheimer flow in the fracture

$$\left(1 + \frac{\beta}{d} |\mathbf{u}_\gamma|\right) \mathbf{u}_\gamma = -K_{f,\tau}\, d\, \nabla_\tau p_\gamma, \quad \operatorname{div}_\tau \mathbf{u}_\gamma = q_\gamma + (\mathbf{u}_1 \cdot \mathbf{n}_1 + \mathbf{u}_2 \cdot \mathbf{n}_2), \quad \text{in } \gamma,$$

with $p_\gamma = 0$ on $\partial\gamma$.

- Impose the interface condition

$$\alpha_\gamma\, p_i = \alpha_\gamma\, p_\gamma + (\xi\, \mathbf{u}_i \cdot \mathbf{n}_i - (1 - \xi)\, \mathbf{u}_{i+1} \cdot \mathbf{n}_{i+1}), \qquad \text{in } \gamma, \text{ for } i = 1, 2,$$

where $\alpha_\gamma = \frac{2K_{f,n}}{d}$, $\xi \in \left(\frac{1}{2}, 1\right]$, and $i + 1 = 1$ if $i = 2$.

N. Frih, J. E. Roberts, A. Saada (2008) Modeling fractures as interfaces: a model for Forchheimer fractures, Comput. Geosci., 12 pp. 91-104.

The weak formulation

We consider the following function spaces:

$$M = L^2(\Omega_1) \times L^2(\Omega_2) \times L^{3/2}(\gamma),$$

$$\mathbf{W} = \{\mathbf{u} = (\mathbf{u}_1, \mathbf{u}_2, \mathbf{u}_\gamma) \in H(\mathrm{div}, \Omega_1) \times H(\mathrm{div}, \Omega_2) \times L^3(\gamma) : \mathrm{div}_\tau \mathbf{u}_\gamma - (\mathbf{u}_1 \cdot \mathbf{n}_1 + \mathbf{u}_2 \cdot \mathbf{n}_2) \in L^3(\gamma),\ \mathbf{u}_i \cdot \mathbf{n}_i \in L^2(\gamma), i = 1, 2\}.$$

- Define the forms $a : \mathbf{W} \times \mathbf{W} \to \mathbb{R}$ and $b : \mathbf{W} \times M \to \mathbb{R}$ by

$$a(\mathbf{u}, \mathbf{v}) = \sum_{i=1}^{2} \left(\mathbf{K}_i^{-1} \mathbf{u}_i, \mathbf{v}_i \right)_{\Omega_i} + \left(\frac{1}{d} \left(1 + \frac{\beta}{d} |\mathbf{u}_\gamma| \right) K_{f,\tau}^{-1} \mathbf{u}_\gamma, \mathbf{v}_\gamma \right)_\gamma + \sum_{i=1}^{2} \left(\alpha_\gamma^{-1} (\xi\, \mathbf{u}_i \cdot \mathbf{n}_i - (1-\xi)\, \mathbf{u}_{i+1} \cdot \mathbf{n}_{i+1}), \mathbf{v}_i \cdot \mathbf{n}_i \right)_\gamma ,$$

$$b(\mathbf{u}, r) = \sum_{i=1}^{2} (\mathrm{div}\, \mathbf{u}_i, r_i)_{\Omega_i} + (\mathrm{div}_\tau\, \mathbf{u}_\gamma, r_\gamma)_\gamma - \left(\sum_{i=1}^{2} \mathbf{u}_i \cdot \mathbf{n}_i, r_\gamma \right)_\gamma .$$

- Define the linear form $L_q : M \to \mathbb{R}$ by:

$$L_q(r) = \sum_{i=1}^{2} (q_i, r_i)_{\Omega_i} + (q_\gamma, r_\gamma)_\gamma .$$

The weak formulation

- The variational problem may be written in standard mixed form as:

$$\text{Find } \mathbf{u} = (\mathbf{u}_1, \mathbf{u}_2, \mathbf{u}_\gamma) \in \mathbf{W},\; p = (p_1, p_2, p_\gamma) \in M \text{ s.t. :}$$

$$\begin{cases} a(\mathbf{u}, \mathbf{v}) - b(\mathbf{v}, p) = 0 & \forall\, \mathbf{v} \in \mathbf{W}, \\ b(\mathbf{u}, r) = L_q(r) & \forall\, r \in M. \end{cases}$$

P. Knabner and J. E. Roberts (2014) Mathematical analysis of a discrete fracture model coupling Darcy flow in the matrix with Darcy-Forchheimer flow in the fracture, ESAIM Math. Model. Numer. Anal., 48 pp. 1451-1472.

Mixed finite element discretization. The algebraic nonlinear system

- We consider again the mixed finite element discretization as before.
- The corresponding algebraic nonlinear system is again a saddle-point problem of the form:

$$\begin{bmatrix} A_1 & C^T & 0 & B_1^T & 0 & F_1^T \\ C^T & A_2 & 0 & 0 & B_2^T & F_2^T \\ 0 & 0 & A_\gamma(U_\gamma) & 0 & 0 & B_\gamma^T \\ B_1 & 0 & 0 & 0 & 0 & 0 \\ 0 & B_2 & 0 & 0 & 0 & 0 \\ F_1 & F_2 & B_\gamma & 0 & 0 & 0 \end{bmatrix} \begin{bmatrix} U_1 \\ U_2 \\ U_\gamma \\ P_1 \\ P_2 \\ P_\gamma \end{bmatrix} = \begin{bmatrix} 0 \\ 0 \\ 0 \\ * \\ * \\ * \end{bmatrix}$$

where A_i, $i = 1, 2$, and $A_\gamma(U_\gamma)$ are diagonal matrices.

The monolithic FAS multigrid method

Let $A_k\, u_k = f_k$ denote a nonlinear system of equations

Full Approximation Scheme (FAS)

- Pre-smoothing: Compute $\bar{u}_k^m$ by applying ν_1 smoothing steps on G^k: $\bar{u}_k^m = S_k^{\nu_1} u_k^m$.
- Restrict the residual and the current approximation to the coarse grid: $r_{k-1} = R_k^{k-1}(f_k - A_k\, \bar{u}_k^m)$, and $u_{k-1}^m = \widetilde{R}_k^{k-1} \bar{u}_k^m$.
- Solve the coarse-grid problem $A_{k-1}(e_{k-1}^m) = A_{k-1}\, u_{k-1}^m + r_{k-1}$.
- Interpolate the error approximation to the fine grid and correct the current fine grid approximation: $\widehat{u}_k^m = \bar{u}_k^m + R_{k-1}^k(e_{k-1}^m - u_{k-1}^m)$.
- Post-smoothing: Compute u_k^{m+1} by applying ν_2 smoothing steps: $u_k^{m+1} = S_k^{\nu_2} \widehat{u}_k^m$.

- If A_h is a linear operator, FAS scheme is identical to the standard linear multigrid method.

Example 7: one fracture with constant permeability

- Dirichlet boundary conditions for the fracture.
- Permeability tensor in the fracture $\mathbf{K} = K_f \, \mathbf{Id}$.
- Forchheimer coefficient $\beta = 10$.

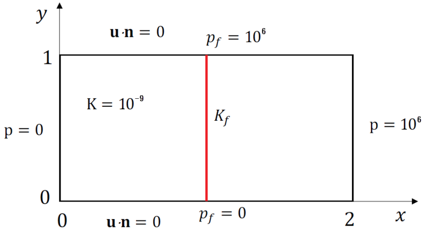

N. Frih, J. E. Roberts, A. Saada (2008) Modeling fractures as interfaces: a model for Forchheimer fractures, Comput. Geosci., 12 pp. 91-104.

Example 7: one fracture with constant permeability

- Pressure distribution for $K_f = 10^{-6}$ (left)
- Convergence of the multigrid method - residual vs. iterations (right)

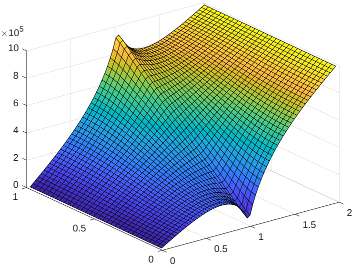

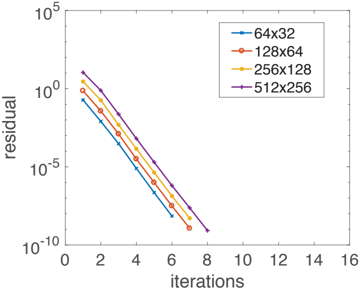

Example 7: one fracture with constant permeability

- We fix the Forchheimer coefficient $\beta = 10$ in order to study the robustness of the mixed-dimensional multigrid method with respect to different values of the permeability of the fracture K_f.

K_f	$h^{-1} = 32$	$h^{-1} = 64$	$h^{-1} = 128$	$h^{-1} = 256$
10^{-6}	8	8	8	9
10^{-4}	9	9	9	9
10^{-2}	9	9	9	10
1	10	10	11	11

Number of $W(2,2)$-iterations of FAS to reduce the initial residual in a factor of 10^{-10}

Example 7: one fracture with constant permeability

- We fix the permeability of the fracture as $K_f = 10^{-6}$, and study the robustness of the mixed-dimensional multigrid method with respect to the Forchheimer coefficient β.

β	$h^{-1} = 32$	$h^{-1} = 64$	$h^{-1} = 128$	$h^{-1} = 256$
0	8	8	8	9
10	8	8	8	9
50	8	9	9	10
100	9	9	10	10
200	10	10	10	10

Number of $W(2,2)$-iterations of FAS to reduce the initial residual in a factor of 10^{-10}

Example 8: two intersecting fractures

- Permeability in the porous matrix $\mathbf{K} = 10^{-6}(1 + xy)\,\mathbf{Id}$ (heterogeneous permeability)
- Permeability tensor in the fracture $\mathbf{K} = K_f\,\mathbf{Id}$.

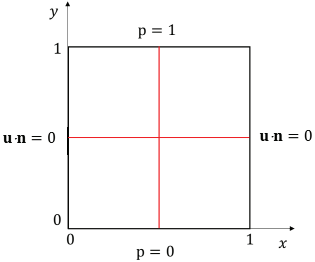

(a) Fracture network and settings

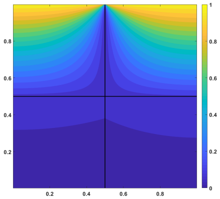

(b) pressure solution for $K_f = 10^{-3}$ and $\beta = 100$

Example 8: two intersecting fractures

- We illustrate the robustness of the proposed algorithm with respect to the permeability in the fracture. The Forchheimer coefficient is fixed to $\beta = 100$.

K_f	$h^{-1} = 32$	$h^{-1} = 64$	$h^{-1} = 128$	$h^{-1} = 256$
10^{-6}	9	9	9	9
10^{-4}	9	9	9	9
10^{-2}	9	9	9	9
1	9	9	9	9

Number of $W(2,2)$-iterations of FAS to reduce the initial residual in a factor of 10^{-10}

Example 8: two intersecting fractures

- We test the robustness of our solver for different values of the Forchheimer parameter. We set the permeability in the fracture to a value $K_f = 10^{-3}$.

β	$h^{-1} = 32$	$h^{-1} = 64$	$h^{-1} = 128$	$h^{-1} = 256$
0	9	9	9	9
10	9	9	9	9
50	9	9	9	9
100	9	9	9	9
200	9	9	9	9

Number of $W(2,2)$-iterations of FAS to reduce the initial residual in a factor of 10^{-10}

Conclusions

MONOLITHIC MULTIGRID METHODS FOR SOLVING:

- Flow problems in deformable porous media (Biot's model) (key: appropriate smoothers)

  F.J. Gaspar, C. Rodrigo, On the fixed-stress split scheme as smoother in multigrid methods for coupling flow and geomechanics, Computer Methods in applied mechanics and engineering 326, 526-540, 2017.

- Coupled flow and porous media problems (key: monolithic approach of both systems + interface conditions)

  P. Luo, C. Rodrigo, F.J. Gaspar, C.W. Oosterlee, Uzawa smoother in multigrid for the coupled porous medium and Stokes flow system,, SIAM Journal on Scientific Computing 39 (5) S633-S661, 2017.

  P. Luo, C. Rodrigo, F.J. Gaspar, C.W. Oosterlee, Monolithic multigrid method for the coupled Stokes flow and deformable porous medium system, Journal of Computational Physics 353, 148-168, 2018.

- Flow problems in fractured porous media (key: mixed-dimensional multigrid components)

  A. Arrarás, F.J. Gaspar, L. Portero, C. Rodrigo, Mixed-dimensional geometric multigrid methods for single-phase flow in fractured porous media. SIAM Journal on Scientific Computing 41 (5) B1082-B1114, 2019.

  A. Arrarás, F.J. Gaspar, L. Portero, C. Rodrigo, Geometric multigrid methods for Darcy-Forchheimer flow in fractured porous media. Computers & Mathematics with Applications 78, 3139-3151, 2019.

Conclusions

MONOLITHIC MULTIGRID METHODS FOR SOLVING:

- Flow problems in deformable porous media (Biot's model) (key: appropriate smoothers)

  F.J. Gaspar, C. Rodrigo, On the fixed-stress split scheme as smoother in multigrid methods for coupling flow and geomechanics, Computer Methods in applied mechanics and engineering 326, 526-540, 2017.

- Coupled flow and porous media problems (key: monolithic approach of both systems + interface conditions)

  P. Luo, C. Rodrigo, F.J. Gaspar, C.W. Oosterlee, Uzawa smoother in multigrid for the coupled porous medium and Stokes flow system,, SIAM Journal on Scientific Computing 39 (5) S633-S661, 2017.

  P. Luo, C. Rodrigo, F.J. Gaspar, C.W. Oosterlee, Monolithic multigrid method for the coupled Stokes flow and deformable porous medium system, Journal of Computational Physics 353, 148-168, 2018.

- Flow problems in fractured porous media (key: mixed-dimensional multigrid components)

  A. Arrarás, F.J. Gaspar, L. Portero, C. Rodrigo, Mixed-dimensional geometric multigrid methods for single-phase flow in fractured porous media. SIAM Journal on Scientific Computing 41 (5) B1082-B1114, 2019.

  A. Arrarás, F.J. Gaspar, L. Portero, C. Rodrigo, Geometric multigrid methods for Darcy-Forchheimer flow in fractured porous media. Computers & Mathematics with Applications 78, 3139-3151, 2019.